

UAS, sensors, and data processing in agroforestry: a review towards practical applications

Luís Pádua, Jakub Vanko, Jonáš Hruška, Telmo Adão, Joaquim J. Sousa, Emanuel Peres & Raul Morais

To cite this article: Luís Pádua, Jakub Vanko, Jonáš Hruška, Telmo Adão, Joaquim J. Sousa, Emanuel Peres & Raul Morais (2017): UAS, sensors, and data processing in agroforestry: a review towards practical applications, International Journal of Remote Sensing, DOI: [10.1080/01431161.2017.1297548](https://doi.org/10.1080/01431161.2017.1297548)

To link to this article: <http://dx.doi.org/10.1080/01431161.2017.1297548>



Published online: 09 Mar 2017.



Submit your article to this journal [↗](#)



Article views: 64




View related articles [↗](#)



View Crossmark data [↗](#)



UAS, sensors, and data processing in agroforestry: a review towards practical applications

Luís Pádua^a, Jakub Vanko^a, Jonáš Hruška^a, Telmo Adão^a, Joaquim J. Sousa ^{a,b}, Emanuel Peres^{a,b} and Raul Morais^{a,b}

^aDepartment of Engineering, School of Sciences and Technology, University of Trás-os-Montes e Alto Douro, Vila Real, Portugal; ^bINESC-TEC (formerly INESC Porto), Porto, Portugal

ABSTRACT

The aim of this study is twofold: first, to present a survey of the actual and most advanced methods related to the use of unmanned aerial systems (UASs) that emerged in the past few years due to the technological advancements that allowed the miniaturization of components, leading to the availability of small-sized unmanned aerial vehicles (UAVs) equipped with Global Navigation Satellite Systems (GNSS) and high quality and cost-effective sensors; second, to advice the target audience – mostly farmers and foresters – how to choose the appropriate UAV and imaging sensor, as well as suitable approaches to get the expected and needed results of using technological tools to extract valuable information about agroforestry systems and its dynamics, according to their parcels' size and crop's types. Following this goal, this work goes beyond a survey regarding UAS and their applications, already made by several authors. It also provides recommendations on how to choose both the best sensor and UAV, in accordance with the required application. Moreover, it presents what can be done with the acquired sensors' data through the use of methods, procedures, algorithms and arithmetic operations. Finally, some recent applications in the agroforestry research area are presented, regarding the main goal of each analysed studies, the used UAV, sensors, and the data processing stage to reach conclusions.

ARTICLE HISTORY

Received 3 October 2016
Accepted 5 February 2017

1. Introduction

Recent years showed rapid socialization and an increased interest in unmanned aircraft system (UAS) for civilian applications. Unmanned aerial vehicles (UAVs), often referred as drone, are aircrafts without a human pilot on board. Instead, UAVs are controlled by a ground operator. This was achieved due to a variety of factors, ranging from the introduction of relatively low-cost systems and user-friendly controls to the general technological advances and to the miniaturization of individual components (main boards, micro-processors and motors, high-power density batteries, cheaper airframes, communication devices, and sensors). These advances led to the production of

affordable off-the-shelf UAS suitable for civilian applications, easy to transport, mount, launch, and operate.

An UAS can be defined as a power-driven reusable aircraft operated without a human pilot on board (Sullivan 2006). It can be remotely piloted or have a programmed route to perform an autonomous flight, using the embedded autopilot. Generally, it also requires a ground-control station, sensor suites and communication devices for carrying out flight missions (Pappalardo 2015).

Apart from military applications (Austin 2010; Gertler 2012; Jenks 2010), the European Parliamentary Research Service provided a list of potential applications in civil and commercial use consisting of disaster response, earth observation, the energy sector, infrastructures, maintenance monitoring, aerial mapping, filming, agriculture, forestry, fisheries, telecommunications, package delivery, and non-military government authorities. In addition, some concerns rose from the increased use of UAS in illegal activities, such as drug trafficking (Juul 2015). The Association for Unmanned Vehicle Systems International (AUVSI) estimates that, among the aforementioned applications, agriculture is at the vanguard of the promising markets for the commercial use of UAS (Jenkins and Vasigh 2013).

In the specific area of agriculture, every farmer's goal is to efficiently apply the available resources to gain the maximum yield possible. To achieve this, they need a fast, reliable, cost-effective, and easy method to scan their fields. The crop's condition can be assessed by the stage of ripening, water status, pest attacks and nutritional requirements. UAS with remote-sensing capabilities can provide this necessary data, so that the farmer is able to identify problems in early stages and rapidly select the appropriate interventions (George et al. 2013). Besides crop monitoring, farmers can also benefit from UAS in precision spraying. Similarly, agriculture, forestry, and nature preservation can also greatly benefit from the use of UAS technology. Foresters can use them for inspection of forestry operations, wildfire detection, wildlife tracking, legal restrictions monitoring, woodland change detection, and survey, sites which are otherwise inaccessible or where trespassing is undesirable (Grenzdörffer, Engel, and Teichert 2008).

There is a wide range of UAS and sensors that can be used in agroforestry, which leaves space for uncertainty among the professionals regarding the use of those devices and how they can actually help to cost-effectively leverage the production. Thereby, the purpose of this study is to help users selecting the proper UAS together with the proper imaging sensor to get the expected and needed results. Several authors already provided surveys regarding UAS and their applications (Colomina and Molina 2014; Nex and Remondino 2013; Pajares 2015; Salamí, Barrado, and Pastor 2014; Watts, Ambrosia, and Hinkley 2012; Zhang and Kovacs 2012). However, in this study authors are focusing on the application of low-cost mini and micro UAS and imaging sensors that meet the interests of both farmers and foresters.

2. UAS as a remote-sensing platform

Remote-sensing platforms are useful to provide added value information for agroforestry applications. This section presents these platforms focusing on UAS, which are classified according to their size. Emphasis is given on small, mini and micro UAS, which are divided in two types: fixed-wing and rotor-based.

2.1. *Traditional remote-sensing technologies and UAS*

Traditional remote-sensing technologies encompass satellite and manned aircraft platforms. These platforms are continuously improving in terms of spatial, spectral, and temporal resolutions. Each of these technologies has benefits and constraints regarding technological, operational and economic factors. The high spatial and temporal resolutions, flexibility and much lower operational costs make UAS a good alternative to traditional remote-sensing platforms for agroforestry applications (Muchiri and Kimathi 2016; Salamí, Barrado, and Pastor 2014).

The use of professional civilian UAS is increasing rapidly around the world, and it is expected to explode in the upcoming years. The main factors supporting this growth are related to the increasing awareness of the benefits that this technology can bring to a wide range of industries and non-commercial sectors, as well as to the introduction of relatively low-cost systems, user-friendly controls and the general technological advancements and the miniaturization of individual components.

According to the AUVSI, the foreseen integration of UAS in the United States national airspace, for the decade 2015–2025, is expected to create more than 100,000 jobs and generate an economic impact of \$82 billion (AUVSI Economic Report 2013).

As a new method of geo-data collection, UAS complements existing techniques, filling the gap between large area imaging (satellites and manned aircrafts), and smaller coverage, time-consuming, but highly accurate terrestrial techniques (Figure 1). Compared to high altitude data, UAS data is fairly low cost, with the advantage that flights can be made often and quickly. UAS are thus very useful when portions of land must be quickly surveyed (quick response capability for, e.g. time-sensitive deliverables, disaster situations or search, and rescue operations). Compared to laser scanning – a very good technique for most of the surveying operations – UAS have the advantage of being above the area to be monitored, which is often a requirement to get an accurate reading. However, and despite the aforementioned advantages of UAS, they are not really competing against traditional aerial photography, since they are seen as a complementary technology.

A technical comparison between multi-rotor UAS, manned aircraft and satellites was made by Matese et al. (2015), to evaluate their cost-effectiveness within the precision agricultural scope. UAS were classified with the best flexibility, optimal cloud cover independence, and regarding the processing tasks, the resolution and precision were also classified as optimal. However, the coverage range, flight endurance, mosaicking, and geocoding effort were classified as poor in comparison with the other two platforms. The case study was implemented in two different vineyards. In heterogeneous vineyards, low-resolution images fail in presenting part of the intra-vineyard variability. The referred study concluded that in small fields (5 ha), rotor-based UAS proved to be the most cost-effective solution. However, and according to the authors' own experience with UAS, fixed-wing small UAVs can be used up to a square kilometre area – with a Ground Sample Distance (GSD) up to 5 cm pixel⁻¹ – and up to 4 km² area for a GSD greater than 10 cm pixel⁻¹. Of course these threshold values depend on the UAS autonomy (the eBee, from SenseFly, was used as reference). It is worth noting that imaging area-coverage is also influenced by flight altitude (directly influences the GSD),






Altitude		Pros	Cons
 Satellite		<ul style="list-style-type: none"> • Extensive coverage • Wide spectral capability 	<ul style="list-style-type: none"> • Low-resolution • Image acquisition timing • Weak coverage in some regions • Sensitive to clouds
	 Manned aircraft	<ul style="list-style-type: none"> • Large coverage with single flight • High-resolution • Wide spectral capability 	<ul style="list-style-type: none"> • Expensive (for small projects) • Image acquisition timing • Weather-dependent • Sensitive to clouds • Not available in remote regions
 Fixed-wing UAV		<ul style="list-style-type: none"> • Cost-effective for small projects • Very high-resolution (fixed wing: up to 2cm/pixel; Rotary: sub-millimetre) • Not affected by clouds due to the lower flight altitude • Positional accuracy 	<ul style="list-style-type: none"> • Small coverage • Regulation may restrict operations • Sensitive to bad weather • Difficult to reconstruct homogenous areas (few tie points)
	 Multi-rotor UAV		
 Terrestrial techniques		<ul style="list-style-type: none"> • Excellent Positional accuracy • Few data (only required) • Very high-resolution • In-situ data classification 	<ul style="list-style-type: none"> • Labour intensive • Only line-of-sight • Accessibility (some sites)

Figure 1. Pros and cons of the existing remote-sensing technologies. Unmanned aerial system (UAS) technology complements existing techniques, filling the existing gap between large-area satellite and manned aircraft imagery and smaller coverage, time-consuming, but highly accurate collection using terrestrial surveying instruments with major pros and cons highlighted.

speed, endurance, and sensor resolution (low resolution sensor lead to lower altitude flights, which impacts on the imaging area).

Therefore, UAS represent an evolution in gathering agricultural and forest statistics data from small to medium areas. Commercial low-cost aerial platforms coupled with high-resolution imaging sensors allow to collect accurate data regarding crop and trees' health at large scale with insignificant clouds' influence (Quiroz 2015).

2.2. UAS main characteristics

The use of UAS equipped with small sensors has emerged as a promising alternative to assist modelling, mapping and monitoring applications in rangelands, forest, and agricultural environments. UASs are also suitable to be used in dirty, dull, and dangerous conditions as wildlife monitoring, ice cover, weather phenomena, and climate change (Watts, Ambrosia, and Hinkley 2012). However, flight regulations and legislation do not always engage technological advancements regarding UAS. Many countries still lack the proper legislation that regulates the use of UAS both for commercial and for leisure purposes. The sooner legislation safely integrates UAS in the airspace – clarifying requirements and conditions under which drones can be operated – the sooner UAS usage will increase. The legal situation with regard to flying a UAS in various different countries is discussed extensively in the paper by Cracknell (2017) which is published in this special issue.

With UAS it is possible to acquire low-cost yet high precision images, since they are acquired from lower altitudes. For agroforestry applications, such level of detail can reveal more information about crop condition, weeds, pests and other abnormalities, leading to an earlier detection. These advantages can help agroforestry professionals in short, medium, and long term operations, due to the possibility of identifying problems faster and, consequently, react quickly, reducing losses, and other economical outlays. Regarding farm management, it is possible to gather more accurate results on how crops are reacting to different treatments, leading to a more effective use of resources.

As previously mentioned, UAS differ in size, physical shape, and operational endurance, which limit the supported payload carrying capacity, operating altitude, and range. This subsection will address UAS of diverse dimensions, but it is important to remind that the main focus of this study are mini and micro UAS, since these types are more affordable, easier to carry and simpler to use than the large- and medium-sized UAS.

Some authors classify UAS in terms of aerospace occupation, altitude, and endurance (Austin 2010; Nex and Remondino 2013; Watts, Ambrosia, and Hinkley 2012; Zhang and Kovacs 2012).

The large UAS used for civilian applications are commonly adapted from military platforms. They are intended to be used on tasks where manned aircraft deployment would be potentially unsafe or inefficient (e.g. in forest wildfires monitoring). NASA's Ikhana UAS (Figure 2(a)) was used to collect and process data regarding fire detection, through a multispectral camera (Ambrosia et al. 2011). These types of platforms require high financial funding, due to the development, deployment and ground operations complexity.

Medium-sized UAS suffer basically from the same problems as large UAS. In comparison, medium-sized UAS feature reduced overall costs and easier take-off/landing operations. An example of a medium-sized UAS is the NASA's SIERRA UAS (Figure 2(b)). It was applied in atmospheric composition, arctic surveys, land cover characterization, surface to air fluxes, disaster response and assessment, agriculture and ecosystem assessment, biological/physical oceanography, island and coastal remote sensing, and coral reef monitoring (Watts, Ambrosia, and Hinkley 2012). Another NASA's UAS, known as Pathfinder-Plus (Figure 2(c)), was applied for surveillance operations and decision support in agriculture, to detect weeds and inconsistencies in the fertilization delivery of coffee plantations, using image acquisition sensors, more specifically RGB and narrow-band multispectral (Herwitz et al. 2004). Due to costs, portability and required

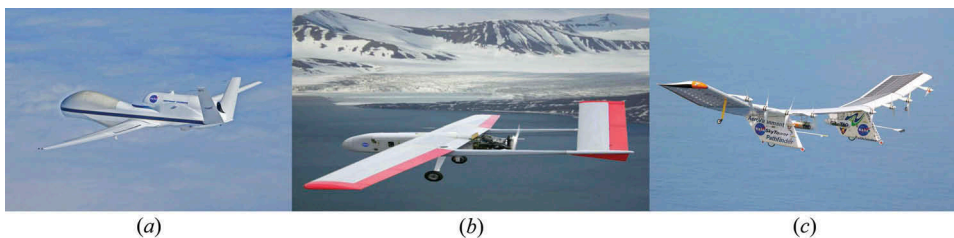


Figure 2. Large and medium-sized unmanned aerial vehicles (UAVs): (a) NASA's Ikhana; (b) NASA's SIERRA; and (c) NASA's Pathfinder-Plus. Image courtesy of NASA.

knowledge for controlling purposes, these types of UAS are not suitable or even affordable for most farmers and foresters.

The small, mini, and micro UAS built for civilian usage features user-friendly platforms, present a typical weight less than 20 kg with a flight time comprised between a couple of minutes and a few hours of autonomy within limited distance range (Hardin and Jensen 2011). Technological advancements have enabled meaningful upgrades to these devices, which are capable of acquiring spatial data in great detail using cost-effective platforms (Watts, Ambrosia, and Hinkley 2012). The expansion of these devices has been facilitated by the miniaturization and the cost reduction of sensors and embedded computers (Berni et al. 2009).

There are two main types of small, micro, and mini UAVs: fixed-wing and multi-rotor. Each type has its own advantages for different deploying environments and required tasks.

The size of the mapped area, its complexity, desired resolution, weather conditions and take-off/landing zone space are the necessary conditions that must be considered before acquiring an UAS. The minimal experience to programme and operate these platforms is an important advantage, given that flight planning and management can be controlled from a single interface.

Fixed-wing UAS can travel several kilometres from the launch point, being mainly suitable for mapping with applications in land surveying, agriculture, mining and environmental management. This type of UAS can achieve a high cruise altitude and speed, cover large areas and get a few centimetres of GSD. However, they are launched by hand or use a small launch ramp and require a large and soft corridor to land. After successful launch, the Global Navigation Satellite System (GNSS) receiver guides, the UAS along a pre-defined path (Hardin and Jensen 2011). The market offers a wide variety of commercial lightweight fixed-wing UAS. Some of the most successful are shown in Figure 3(a–e).

The multi-rotor UAS rely on a set of propellers arranged around its core (Figure 4(a–e)) being the most suitable for inspection, surveying, construction, emergency response, law enforcement and cinematography, and videography. Their low cruise altitude and speed



Figure 3. Some of the most representative fixed-wing UAVs: (a) QuestUAV Q-Pod; (b) SenseFly eBee; (c) Trimble UX5; (d) MAVinci Sirius Pro; and (e) PrecisionHawk Lancaster. The images were obtained from the manufacturers' websites.

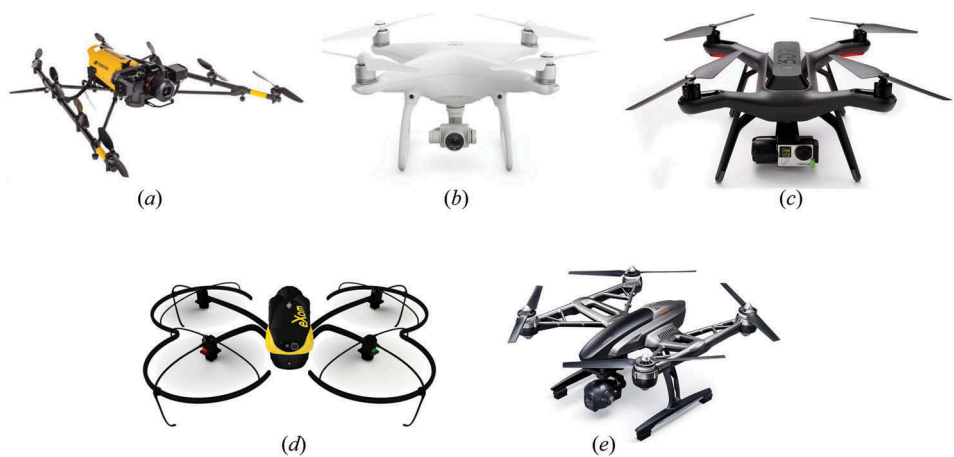


Figure 4. Some of the most representative rotor-based UAVs: (a) Topcon Falcon 8; (b) DJI Phantom 4; (c) 3DR SOLO Quadcopter; (d) SenseFly eXom; and (e) Yuneec Typhoon. The images were obtained from the manufacturers’ websites.

are adequate to cover small areas, obtaining spatial resolution up to 1 mm GSD. Moreover, their vertical take-off and landing (VTOL) only requires a few square metres of free terrain, contrarily to fixed-wing-based systems. The rotors can be arranged around the UAV or can be attached to a set of fixed arms. Multi-rotors are less prone to vibrations than fixed-wing Wallace et al. (2011). As more rotors are added, the lesser is the crash risk and heavier payloads are supported, although the payload size limitation remains (Anderson and Gaston 2013).

Regarding mini and micro UAVs, a few considerations should be made before acquiring or deploying them. Anderson and Gaston (2013) presented the four main constraints for consideration: (1) platform; (2) sensor; (3) operating; and (4) environmental constrains. Table 1 summarizes the major differences between the fixed-wing and the multi-rotor UAVs.

There are two approaches to carry out a UAS mission: by autopilot according to a predefined flight path or manually with a remote controller operated by a pilot. An autonomous flight can be achieved in the following main steps: (1) flight plan – most of

Table 1. Comparison between mini and micro fixed-wing and rotor-based UAVs regarding specific parameters and examples of tasks that can be performed.

	Fixed-wing	Multi-rotor
Image resolution	Up to centimetre level	Up to millimetre level
Take-off	Hand/small launch ramp	Vertical take-off
Payload capacity	Small	Depending on the number of rotors
Flight time	High (usually up to 1 h)	Low (usually up to 30 min)
Landing surface	Several metres of extension	Approximately the UAV size
Coverage	Fixed-wing outperforms multi-rotor, most of the times	
Cruise speed		
Wind resistance		
Main applications	Land surveying, agriculture, GIS, mining, environmental management	Inspection, video, surveying (urban scale), construction and emergency

the recent UAS are released with a flight planning software, and there are also freely available smartphone applications that allow to specify the intended area of interest, mark the launch area (i.e. where the UAV will gain enough altitude to start the mission) and the landing area; (2) after planning – the flight path must be uploaded to the UAV, making it available to start the next step, the flight execution and data gathering. After a successful launch, the UAV will automatically capture images triggered using the GNSS location as reference. Sufficient overlap of the images ensures enough redundant data in case of distorted images; (3) after landing – the obtained data are downloaded and later processed in a software that provides the desired output; and (4) the last step is to evaluate the data, for the intended purpose (e.g. field issues, irrigation issues, water stressed crops, crop height).

As previously mentioned, lightweight UAVs have limited payload, which makes most of the available platforms unable of carrying a multi-sensor system. In some cases, to acquire data from different sensors, the UAV must perform multiple flights over the same area.

The next section provides the different types of sensors used in UAS flight missions.

3. Sensors

The critical component for carrying out remote-sensing activities is the imaging or sensing payload which defines the capabilities and the usability of the UAV (Siebert and Teizer 2014). The current huge market offer of imaging sensors can be quite overwhelming at first glance for a non-expert user. To help farmers and foresters making their final decision, an overview of imaging sensor types is provided together with their main applications in precision agriculture and forestry. It is noteworthy that the development of UAVs and sensors occurs at a rapid rate which, expectedly should not slow down in the upcoming years (Wagner 2015). In the near future, most of the current systems will probably be discontinued, evolve or be replaced by entirely new systems. Therefore, potential buyers should always find up-to-date information about the current state of available UAVs and sensing instruments. UAVs as a remote-sensing platform are capable of carrying a large variety of sensors, from low-cost commercial digital single-lens reflex (DSLR) cameras to expensive professional gear, such as hyperspectral cameras or lidar sensors, specially designed for UAVs (Klemas 2015).

Each remote-sensing device detects a portion of the electromagnetic radiation. Gamma rays, x-rays, ultraviolet, visible light, infrared light, microwaves, and radio waves are examples of electromagnetic radiation that differ from each other concerning wavelength. This range of electromagnetic radiation is called the electromagnetic (EM) spectrum. Only a very small portion of the EM spectrum is visible by the (naked) human eye. However, some sensors can detect different parts of the EM spectrum allowing humans beings to interpret it and therefore make the non-visible become visible. In this study, two types of imaging sensors will be discussed: passive and active sensors.

Passive sensors are used for natural emissions detection from the Earth's surface and its atmosphere whereas active sensors transmit their own pulses of radiation from their own source of energy and then detect the incoming reflected radiation. Passive sensors include RGB cameras, near-infrared (NIR) cameras, thermal cameras, and their combinations in multispectral and hyperspectral cameras, while lidar and radio detection and

ranging (RADAR) are examples of active sensors (Richards and Jia 2006; Turner et al. 2003).

3.1. RGB sensors

Visible light sensors are capable of capturing imagery perceptible to the human eye. Optical visible light cameras operate in the wavelength range, approximately, from 400 to 700 nm (Austin 2010). UAVs can benefit from a large scale of mass-market off-the-shelf cameras to professional grade cameras with prices varying accordingly. In their review, Colomina and Molina (2014) present a list of small and medium format visible band cameras with their basic parameters. In addition to this list, Figure 5(a–e) display some currently used RGB cameras suitable for mini and micro drones, for agricultural and forestry applications.

RGB sensors mounted on UAVs are capable of providing high-resolution imagery from a bird's eye perspective, as presented in Figure 6. These images can be processed into orthophotograph mosaics, by stitching images together (Turner, Lucieer, and Watson 2012), or to build digital surface models (DSMs), using three-dimensional (3D) reconstruction algorithms based on stereo vision or structure from motion (SfM) algorithms (Nex and Remondino 2013). Possible uses of orthophotograph mosaics include aerial mapping and imaging, plant counting, surveillance, emergency response, surveying, and land-use applications. DSMs can be useful for 3D surveying and mapping or volume computation.

Remote-sensing applications also very often separate RGB channels and work with individual red, green, and blue channels. Colour reassigning is used to create false colour images to enhance certain features that can be very useful in land analysis. While this kind of imagery might provide valuable visual information for farmers and foresters, it is not very suitable to assess vegetation properties due to the lack of information obtained in the NIR region, where the high reflectance of vegetation occurs (Nebiker et al. 2008).

3.2. Infrared sensors

The infrared spectrum covers longer wavelengths than the visible light spectrum, ranging from around 700 nm (NIR) to 100,000 nm (far infra-red, FIR). The boundaries between the visible and NIR, at one end, and between the FIR and microwaves, on the other end, are not precise and are open to different interpretations (Austin 2010b). The NIR band from 700 nm to approximately 8500 nm represents the region where high



Figure 5. Examples of optical cameras commonly used on UAVs for RGB image acquisition: (a) GoPro Hero 4 Black edition; (b) Canon G9X; (c) Panasonic Lumix DMC-TZ71; (d) Sony Alpha 7; and (e) Nikon D800.

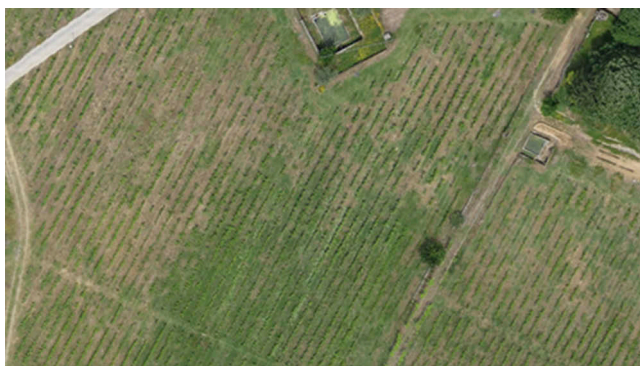


Figure 6. RGB image sample obtained with Sensefly's eBee fixed-wing UAV over one of the University of-Trás-os-Montes e Alto Douro (UTAD) vineyard.

plant reflectance occurs, thus being crucial for most of the agroforestry applications. An NIR image is displayed in [Figure 7](#).

NIR sensors are frequently used in precision agriculture applications and constitute the basis for vegetation analysis. Healthy vegetation that is actively growing and producing energy from photosynthesis reflects more in the NIR region. When combined with RGB, it can be used for vegetation indices (VIs) calculations which are based on the fact that vegetation reflects various wavelengths differently. Most of the common off-the-shelf cameras have filters blocking NIR. However, it is relatively easy to transform a RGB camera into a NIR camera, by removing the filter and replacing it by one that is filtering the visible red, green or blue bands. [Figure 8\(a-c\)](#) display some of currently used cameras that were converted to NIR cameras by changing the filters. NIR and RGB sensors are often combined in multispectral sensors, which will be addressed later.

While the human eye is less sensitive to NIR, FIR is entirely invisible for us. With the intensity increase, this radiation can be experienced as heat. Thermal cameras operate approximately in the spectrum at wavelengths from 5000 to 14,000 nm. Each pixel's intensity can be transformed into a temperature measurement.



Figure 7. NIR image sample obtained with Sensefly's eBee fixed-wing UAV corresponding to the same area represented in 'figure 6'.



Figure 8. NIR cameras commonly used in UAVs: (a) Canon S110; (b) Panasonic Lumix 7; and (c) Fujifilm X-M1.



Figure 9. Common thermal cameras developed to be mounted on UAVs: (a) Workswell WIRIS and (b) FLIR Vue.

When compared with conventional cameras, thermal cameras are much more expensive and the image resolution is much lower (Mejias, Lai, and Bruggemann 2015). Thermal sensors allow to create full thermal maps (Lagüela et al. 2015), to check irrigation management (Gonzalez-Dugo et al. 2013), to assess the functionality of solar panels (Quater et al. 2014) and to detect wildlife or livestock (Israel 2011). A couple of thermal cameras developed for UAS are depicted in Figure 9(a–b).

3.3. Multispectral and hyperspectral sensors

Until a few years ago multispectral and hyperspectral cameras were considered too heavy for mini and micro UAVs, whereas RGB and modified RGB cameras, for acquiring the NIR band, were considered as a standard tool coupled with UAVs for photogrammetric and remote-sensing applications. Apart from early prototypes (Saari et al. 2011), such cameras only became commercially available in recent years. Just like NIR sensors, multispectral sensors are extensively used for vegetation analysis, since NIR is one of the multiple bands they can detect (usually R, G, B, NIR, red edge, and sometimes ultraviolet light and thermal bands are included in multispectral sensors). Red edge refers to the EM region between visible light spectrum and NIR. Some of the most used multispectral sensors are shown in Figure 10(a–d). Nebiker et al. (2016) made a comparison between a high-end multispectral camera and a low-cost off-the-shelf NIR camera showing



Figure 10. Some of the most commonly used multispectral cameras: (a) Parrot Sequoia; (b) multiSPEC 4C; (c) Tetracam ADC; and (d) MicaSense RedEdge.

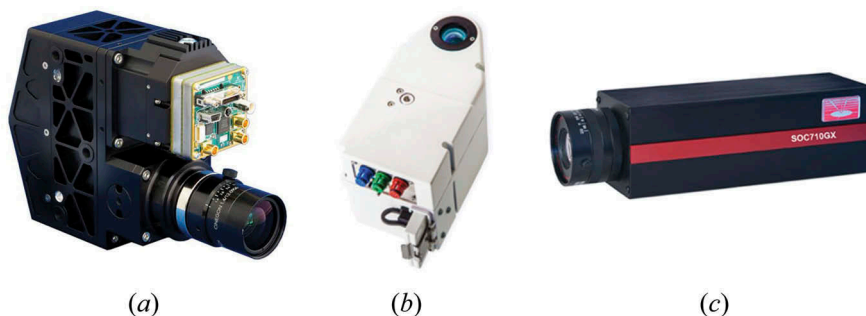


Figure 11. Some of the most common used hyperspectral cameras: (a) the Headwall Photonics Micro-Hyperspec; (b) the Rikola Hyperspectral camera; and (c) the Surface Optics Corp. SOC7100-GX.

significant differences. As expected, the multispectral sensor provided good results, consistent with the reference values obtained by a hyperspectral spectrometer while the low-cost camera showed a reasonable correlation with the multispectral system with some significant biases. However, the use of high spatial resolution low-cost cameras proved to be useful for qualitative monitoring of crops, including diseases detection.

While multispectral cameras sense broadbands, usually 4–12, hyperspectral cameras (Figure 11(a–c)) are capable of sensing hundreds of narrow bands, up to 2 nm in wavelength (Bendig 2015).

Hyperspectral sensors produce images in which each pixel contains the whole spectrum of the sensed wavelengths. This means that hyperspectral outcomes provide much more information than the imagery produced by the previously referred devices. A simplified representation of a hyperspectral data cube is shown in Figure 12. A list of both multispectral and hyperspectral sensors used in conjunction with UAVs in several published works can be found in the work of Colomina and Molina (2014).

3.4. Lidar sensors

Lidar is an active laser-based remote-sensing technology that transmits to the surface optical laser pulses with a fast repeat rate. By measuring the double path time from the emitted pulse (transmitter–target–transmitter/receptor), it is possible to determine the distance to targets (objects, surface). By repeating this process with a fast sequence, lidar generates a 3D point cloud of the surface, as shown in Figure 13.

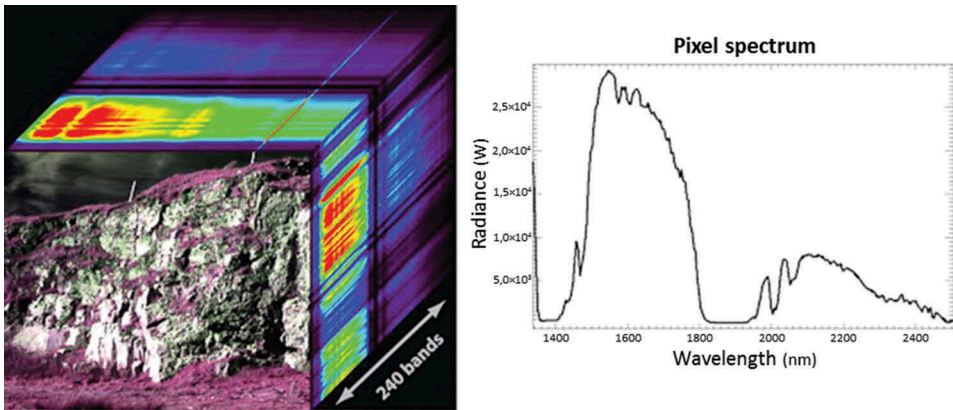


Figure 12. Two-dimensional projection of a hyperspectral data cube. The high number – typically, over 100 – of narrow spectral bands results in a continuous range of reflectance values for each image pixel. The front of the cube shows a false colour image using the infrared spectral bands 1721, 2306, and 1565 nm in RGB (image from <http://org.uib.no/cipr/Project/VOG/hyperspectral.htm>).

The accuracy of these 3D point clouds allows them to be used for multiple applications in agroforestry, forest change detection (Wallace, Lucieir, and Watson 2014), flood mapping (Malinowski et al. 2016), or plant height measurements (Bareth et al. 2016). Short-range lidar sensors were also used on-board UAVs for obstacle detection and guidance (Ramasamy et al. 2016). In the near future, further miniaturization and cost

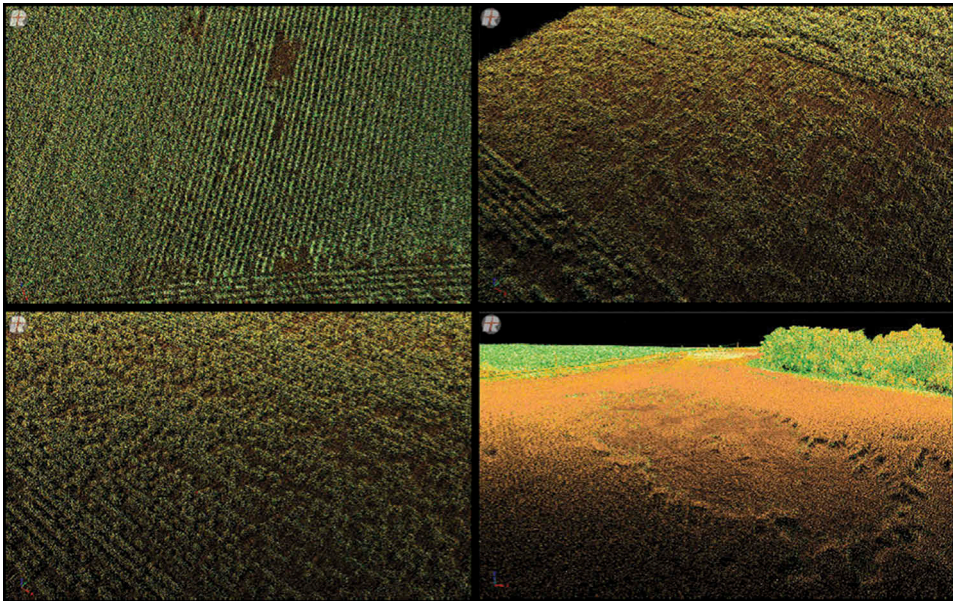


Figure 13. UAV-based lidar data of different agriculture features (Amon et al. 2015). Properly sparse surveys in time provide valuable data to detect cropland critical areas. © RIEGL LMS, www.riegl.com

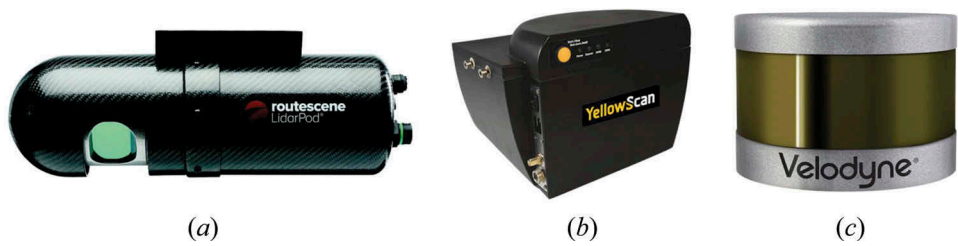


Figure 14. Examples of commonly used UAS lidar sensors: (a) the Rousescene lidar Pod; (b) the Yellowscan Mapper; and (c) the Velodyne PUCK.

reduction of lidar sensors is expected (Poulton and Watts 2016). Figure 14(a–c) show some currently available lidar systems suitable for UAS.

Table 2 presents some examples of application areas and studies in which the described sensors were used. Depending on the goal of certain applications, the sensor should be properly selected, considering the trade-off between characteristics and goals to reach. Thermal sensors provide spectral bands that are more suitable for applications that require temperature information invariant to light conditions as, for example, real-time animal detection. Disease detection, in early stages, can be performed by hyperspectral sensors since many of them only present slightly noticeable visible characteristics. On the other hand, and despite of the fact that some similar tasks can be achieved with thermal and hyperspectral sensors, such as water status assessment, other aspects need to be considered (e.g. spatial

Table 2. List of potential application areas with examples of scientific studies, grouped by sensor type.

Sensors	Application areas	References
RGB	Forest canopy gaps inspection	Getzin, Wiegand, and Schöning (2012)
	Biomass monitoring	Bendig et al. (2014)
	Volume characterization	Ballesteros et al. (2015)
	Vegetation segmentation	Nolan et al. (2015)
	Early-season crop monitoring	Torres-Sánchez et al. (2014); Gómez-Candón, Castro, and López-Granados (2013)
Thermal	Land-use classification	Lagüela et al. (2015)
	Water status assessment	Baluja et al. (2012); Zarco-Tejada, González-Dugo, and Berni (2012); Park et al. (2015)
	Wildlife detection	Israel (2011); Ward et al. (2016)
	Irrigation management	Bellvert and Girona (2012); Bellvert et al. (2013)
	Fire detection	Merino et al. (2011)
Multispectral	Vigour maps production based on vegetation indices (VIs)	Primicerio et al. (2012); Candiago et al. (2015); Nebiker et al. (2008); Navia et al. (2016)
	Image segmentation	Comba et al. (2015)
	Weed mapping	Peña et al. (2013)
	Nitrogen status estimation	Caturegli et al. (2016)
	Biomass estimation	Bendig et al. (2015)
Hyperspectral	Biomass estimation	Honkavaara et al. (2012); Pölönen et al. (2013)
	Chlorophyll estimation	Uto et al. (2013)
	Nitrogen status estimation	Pölönen et al. (2013)
	Water status assessment	Zarco-Tejada, González-Dugo, and Berni (2012)
	Early detection of plant disease	Calderón, Navas-Cortés, and Zarco-Tejada (2015)
Lidar	Bellow forest canopy mapping	Chisholm et al. (2013)
	Forest inventory and structural properties	Wallace et al. (2012); Wallace (2013); Wallace et al. (2016)
	Assessment of tree parameters	Park et al. (2015)

and spectral resolution and acquisition costs). These topics are addressed in [Section 5](#) of this study, where the estimated budgets of UAS bundles for different agroforestry applications are also presented (including UAV platform, sensors, and processing software).

The amount of data collected by sensors mounted on UAVs can be huge, prompting the need for methods able to transform them into valuable information. In the next section this topic is addressed.

4. Data processing

After each flight, the sensors mounted on the UAV returns a large amount of data, which is not yet suitable to extract information and to reach conclusions, since platforms are rarely designed to interact on-the-fly with the attached sensors. Thus, the desired results must be pursued in a post-flight processing stage (Geipel et al. 2013). This section intends to present the several operations that can be performed with the acquired data, in the referred post-flight processing stage.

4.1. Image pre-processing

Numerous issues may affect data quality. To enhance the data, a pre-processing stage is commonly used. Issues such as atmospheric distortions, spectral variability of the surface materials, altitude, wind turbulence, camera focal length and viewing angle are external factors that may contribute to image degradation. For these reasons, to detect changes as revealed by modifications in surface reflectance and to be able to compare acquired data in different epochs (time-series analysis), it is necessary to carry out radiometric corrections. Two approaches to radiometric calibration are possible: (1) ground measurements at the time of data acquisition for atmospheric correction and sensor calibration; and (2) radiometric calibration target that allows the user to calibrate and correct the images' reflectance, considering the illumination and some of the sensor's characteristics. It is recommended to use such a target when generating index maps. Practically, the radiometric calibration target is a white balance card. The radiometric calibration target should cover enough pixels to get good statistics.

In most use cases, a single image cannot cover the entire area of interest, which makes it necessary to capture several overlapping images of the area ([Figure 15\(a\)](#)). These images have to be stitched together into a single orthophotograph mosaic ([Figure 15\(b\)](#)). Jia et al. (2015) describe the mosaicking process based on the scale-invariant feature transform (SIFT) algorithm. The process can be subdivided into the following steps: (1) image pre-processing; (2) image registration (feature extraction, feature matching, model transformation, and parameter estimation); and (3) image fusion. In addition, the correction of the image's geolocation can be achieved with ground control points (GCPs).

It should be noticed that the most common UAS limit the sensor payload in weight and dimension, imposing the selection of standard small format sensors for imaging. The sensor's characteristics (focal length changes, principal point offset, lens optical distortion, etc.) along with external factors produce image deformations. The cause of resolving the above parameters is called geometric calibration, which is critical to ensure



Figure 15. Ortophomoaig generation example. (a) Images gathered in a UAV flight over UTAD's campus. (b) Orthorectified image mosaic which is the result of the processing operations (involving homographic corrections and stitching) upon the acquired images.

UAS's data geolocation precision and significant for UAS quantitative remote-sensing application.

4.2. Spectral indices

To easily extract information from the mosaic, there are different spectral indices that can be applied. These indices are calculated through the use of information about the surface's reflectance from two or more wavelengths or spectral bands. The results provide a relative abundance of certain features. The mostly used indices are VIs. However, other available types of indices can be useful for agroforestry professionals, e.g. burned areas and water or snow indices.

VIs are not recent and were used in the evaluation of data gathered by other remote-sensing platforms (e.g. satellites) before being applied to UAS data. Its use extends from crop and vegetation monitoring to estimation of plant parameters.

There are broad and narrowband indices, both designed to measure the overall amount and quality of photosynthetic material, which is crucial for understanding vegetation's state. Broadband greenness VIs are the simplest way to measure the general quantity and vigour of green vegetation. Narrowband greenness VIs are intended for use with imaging spectrometers, making them suitable for precision agriculture since these can be used to identify, analyse and manage. Comparing both types, narrowband VIs are more sensitive to smaller changes in vegetation health, mainly in areas with dense vegetation where broadband measures can saturate.

Vegetation detection through images is possible due to the absorption of red and blue channels and a higher reflectance of the green and NIR channels. Different spectral signatures are obtained from different vegetation types concerning size, shape, and colour of leaves (Salamí, Barrado, and Pastor 2014).

VIs can also be used to calculate biomass, leaf area index (LAI), disease detection, water stress presence, and nitrogen content, assisting farmers and foresters in crop management, yield forecasting and environmental protection (Zhang and Kovacs 2012). Series of used VIs can be found in the works of Baluja et al. (2012), Gnyp et al. (2014), López-López et al. (2016), Salamí, Barrado, and Pastor (2014), Zarco-Tejada et al. (2005). NIR VIs are reported to have a good correlation with biomass and LAI (Thenkabail, Smith, and De Pauw 2000). López-López et al. (2016) have separated some VIs in different categories: structural indices, pigment indices or chlorophyll $a + b$ indices, carotenoid indices, xanthophyll indices, R/G/B indices, chlorophyll fluorescence, and plant disease index. Table 3 provides the necessary information about the most commonly used VI, including the formula allowing their calculation and their main applications. Theoretical basis regarding the VI are provided by Galiano (2012) mostly related to water stress VIs.

Indices based on NIR and visible spectrum combine NIR and red bands for biomass estimation, canopy structure, and LAI. Among them, the most commonly used index is the normalized difference vegetation index (NDVI) (Zhang and Kovacs 2012) proposed by Rouse et al. (1974). Figure 16 presents a false colour image obtained after NDVI calculation from a vineyard.

Wehrhan, Rauneker, and Sommer (2016) compared different VIs (NDVI, transformed soil-adjusted vegetation index, and enhanced vegetation index (EVI)) to the plant-related carbon dynamics in agricultural soils using a fixed-wing UAV with a multispectral camera array. EVI was pointed out as the best correlation index between ground-based measurements of fresh phytomass.

With the use of visible band indices, it is also possible to acquire vegetation parameters. (Bendig et al. 2015) showed that the visible band indices (GRVI, MGRVI, RGBVI) presented a better ability to model biomass in early growth stages rather than later ones, achieving a cost-effective alternative for ground-based reflectance measurements.

Torres-Sánchez et al. (2014) compared different visible spectrum VIs: ExG (Woebbecke et al. 1995), ExGR, Woebbecke index (Woebbecke et al. 1995), normalized green–red difference index (NGRDI) (Gitelson et al. 2002), vegetative (VEG) (Hague, Tillet, and Wheeler 2006), and two VI combinations in two different flight altitudes (30 and 60 m)

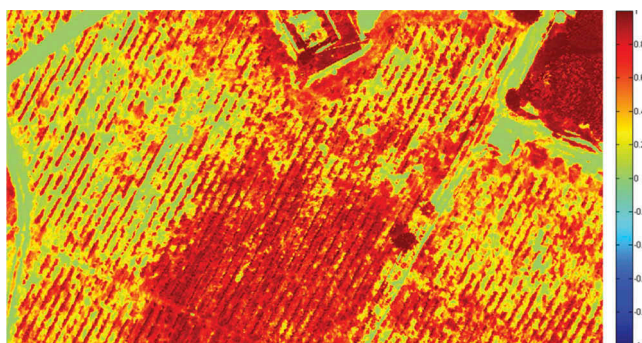


Figure 16. False-colour representation of a normalized difference vegetation index (NDVI) image composed of red and near-infrared (NIR) bands corresponding to 'Figures 5–6'.

Table 3. Case-study applications, grouped by vegetation index (VI) and respective formulas, operating bands and literature references.

Index	Name	Formula	Bands	Reference	Applications/description
Vis					
CWSI	Crop water stress index	$CWSI = \frac{T_{canopy} - T_{wet}}{T_{dry} - T_{wet}}$	Thermal	Idso et al. (1981)	Analysis of plant hydration, given by the difference between the measured canopy temperature and a non-water-stressed baseline and diseases identification in early stage (Salami, Barrado, and Pastor 2014) Used for generate maps that help in precision irrigation management in vineyards (Bellvert et al. 2013) and to assess the spatial variability of tree water status on heterogeneous orchards (Bellvert et al. 2016; Park et al. 2015)
lg	Stomatal conductance index lg	$lg = \frac{T_{dry} - T_{canopy}}{T_{canopy} - T_{wet}}$	Thermal	Jones (1999)	Uses thermal bands in combination with wet and dry surface references to address environmental variations. Depending on the humidity and canopy height the results cannot be notorious, i.e. small temperature variations
l3	Stomatal conductance index l3	$l3 = \frac{T_{canopy} - T_{wet}}{T_{dry} - T_{canopy}}$	Thermal		
NDVI	Normalized difference vegetation index	$NDVI = \frac{NIR - Red}{NIR + Red}$	NIR RGB	Rouse et al. (1974)	Biomass estimation (Bendig et al. 2015), canopy structure, Leaf Area Index and crop management (Candiago et al. 2015)
SAVI	Soil-adjusted vegetation index	$SAVI = \frac{NIR - Red}{NIR + Red + 1} + L$	NIR RGB	Huete (1988)	(Depending on the season of the year this may not be suitable due to leaf colour change, since the reflectance from the green band is not used in index calculation)
MSAVI	Modified soil-adjusted vegetation index	$MSAVI = \frac{NIR - Red + 1}{NIR + Red + 1}$	NIR RGB	Qi et al. (1994)	Biomass estimation (Bendig et al. 2015), canopy structure, leaf area index, and crop management (Gitelson, Kaufman, and Merzlyak 1996)
OSAVI	Optimized soil-adjusted vegetation index	$OSAVI = \frac{1.5NIR - Red}{NIR + Red + 0.6}$	NIR RGB	Rondeaux, Steven, and Baret (1996)	(These indices are based on NDVI but aim the minimization of soil brightness variations)
TCARI	Transformed chlorophyll absorption ratio index	$TCARI = 3 \left[(R_{700} - R_{670}) - 0.2(R_{700} - R_{550}) \left(\frac{R_{700}}{R_{670}} \right) \right]$	Red edge Red	Haboudane et al. (2002)	Access vine water status (Baluja et al. 2012), separating of vegetation from soil background, (Perez et al. 2000). If normalized by the optimized soil-adjusted vegetation index (TCARI/OSAVI) integrates advantages of the minimization of soil background effects (OSAVI) and chlorophyll concentration estimation (TCARI) (Haboudane et al. 2002)

(Continued)

Table 3. (Continued).

Index	Name	Formula	Bands	Reference	Applications/description
GNDVI	Green normalized difference vegetation index	$GNDVI = \frac{NIR - Green}{NIR + Green}$	NIR RGB	Gitelson, Kaufman, and Merzlyak (1996)	Crop management (Gitelson, Kaufman, and Merzlyak 1996)
DVI	Difference vegetation index	$DVI = NIR - Red$	NIR RGB	Tucker (1979)	
EVI	Enhanced vegetation index	$EVI = G \left(\frac{NIR - Red}{NIR + G_1 Red + G_2 Blue + L} \right)$	NIR RGB	Justice et al. (1998)	Leaf Area Index (where NDVI may saturate. It reduces atmospheric influences by adding the blue band combined with the red band and NIR reflectance)
RVI or PCDI	Ratio vegetation index or plant cell density index	$RVI \text{ or } PCDI = \frac{NIR}{Red}$	NIR RGB	Jordan (1969)	Used to measure vine vigour (Bramley and Hamilton 2007)
GRVI NDI NGRVI	Green red vegetation index	$GRVI = \frac{Green - Red}{Green + Red}$	RGB	Falkowski et al. (2005), Gitelson et al. (2002), Perez et al. (2000), Tucker (1979)	Marker for green vegetation, soils, water/snow, phonological indicator, separating of vegetation from soil background (Motohka et al. 2010)
MGRVI	Modified green red vegetation index	$MGRVI = \frac{Green^2 - Red^2}{Green^2 + Red^2}$	RGB	Bendig et al. (2015)	Barley biomass monitoring (Gnyp et al. 2014)
RGBVI	Red green blue vegetation index	$RGBVI = \frac{Green^2 - BlueRed}{Green^2 + BlueRed}$	RGB	Bendig et al. (2015)	
BGVI	Blue/green pigment index	$BGVI = \frac{Blue}{Green}$	RGB	Zarco-Tejada et al. (2005)	Water stress detection
BRVI	Blue/red pigment index	$BGVI = \frac{Blue}{Red}$	RGB	Zarco-Tejada et al. (2005)	
ExG	Excess green	$ExG = 2Green - Red - Blue$	RGB	Woebbecke et al. (1995)	Early-season crop detection (Torres-Sánchez, López-Granados, and Peña 2015; Torres-Sánchez et al. 2014)
ExG-R	Excess green red	$ExG - R = ExG - 1.4Red - Green$	RGB	Neto (2004)	Wheat field monitoring (Hague, Tillett, and Wheeler 2006)
VEG	Vegetative	$VEG = \frac{Green}{Red^2 Blue^{(1-a)}} \text{ with } a = 0.667$	RGB	Hague, Tillett, and Wheeler (2006)	
PRI	Photochemical reflectance index	$PRI = \frac{R_{841} - R_{670}}{R_{841} + R_{670}}$	RGB	Gamon, Peñuelas, and Field (1992)	It uses visible range images and is related to changes in photosynthetic efficiency. PRI is computed by the use of narrowband reflectance (R) at 531 and 570 nm wavelength. Berni et al. (2009) used PRI to investigate water stress in citrus orchard

(Continued)

Table 3. (Continued).

Index	Name	Formula	Bands	Reference	Applications/description
PCDI	Plant cell density index	$PCDI = \frac{NIR}{Red}$	RGB	Bramley and Hamilton (2007)	Represents the ratio between NIR and red bands and can be used to measure of vine vigour (Bramley and Hamilton 2007). It was also applied multispectral and thermal imagery to evaluate the relationship between grapevine water status and PCDI and CWSI Bellvert and Girona 2012). PCDI can be useful to discriminate well-watered zones in a vineyard as well as acting as a tool for irrigation scheduling
GnyLi index	Named by the developers Gny and Li	$GnyLi = \frac{R_{900}R_{1050} - R_{900}R_{1220}}{R_{900}R_{1050} + R_{900}R_{1220}}$	NIR	Gnyp et al. (2014)	Barley biomass monitoring (Gnyp et al. 2014)
Burn indices					
BAI	Burn area index	$BAI = \frac{1}{0.1 - Red^2 + 0.06 - NIR^2}$	NIR RGB	Martín Isabel, Del and Chuvieco Salinero (1998)	Uses the NIR and red spectrum bands to highlight the burned land in post-fire images (Martín Isabel, Del, and Chuvieco Salinero 1998)
NBR	Normalized burn ratio	$NBR = \frac{NIR - SWIR}{NIR + SWIR}$	NIR SWIR	García and Caselles (1991)	Similar to NDVI index, but it uses the shortwave infrared (SWIR) instead of the red band (García and Caselles 1991) to identify the darker pixels representing burned areas. It is suitable to calculate burned parts in areas greater than 200 ha
NBRT	Normalized burn ratio – thermal	$NBRT = \frac{NIR - SWIR \left(\frac{Thermal}{1000} \right)}{NIR + SWIR \left(\frac{Thermal}{1000} \right)}$	Thermal NIR SWIR	Holden et al. (2005)	Uses the thermal band that improves the differentiation between burned and unburned land (Holden et al. 2005)
Miscellaneous indices					
NDSI	Normalized difference snow index	$NDSI = \frac{Green - NIR}{Green + NIR}$	RGB NIR	Riggs, Hall, and Salomonson (1994)	Used to detect snow
NDWI	Normalized difference water index	$NDWI = \frac{NIR - SWIR}{NIR + SWIR}$	NIR SWIR	Gao (1996)	Used to detect and enhance the presence of water in images: NDWI is similar to NBR, however, values close to 1 represent areas with a strong presence of water. MNDWI uses the green band instead of NIR to improve the NDWI results, enhancing water features

using multiple flights during the early season in a wheat field, among them ExG and VEG achieved the best performance.

The need to identify diseases in early stage is crucial to provide a proper crop protection. Regarding this topic, Salamí, Barrado, and Pastor (2014) concluded that indices based on crown temperature (CWSI) and visible ratio indices proved to be effective. Calderón, Navas-Cortés, and Zarco-Tejada (2015) used classification methods (linear discriminant analysis (LDA) and Support Vector Machine (SVM)) to classify the verticillium wilt severity on olives through hyperspectral and thermal imagery data. SVM achieved better overall results than LDA. However, LDA is more effective for initial and low severity disease levels. The type of indices that suited better for verticillium wilt identification were normalized canopy temperature, chlorophyll fluorescence, structural, xanthophyll, chlorophyll, carotenoid, and disease indices. A similar study was conducted by López-López et al. (2016) to evaluate disease incidence and severity in almond orchards affected by the red leaf blotch fungal. Several indices were described and used to detect disease symptoms: the better results were achieved by pigment indices (chlorophyll $a + b$ indices) and chlorophyll fluorescence in disease and severity detection, making them appropriate for decision support and implementation of precision crop protection techniques. Thermal imagery can be used to detect low transpiration rates caused by root diseases.

Burn indices have been useful for forestry professionals, land resource managers and fire officials to estimate areas of potential fire hazards, fire perimeter mapping and study and measure post-fire burn and vegetation regrowth areas. In this type of indices, a pre-processing stage is needed in order to mask water presence in the images. Chuvieco, Martín, and Palacios (2002) compared different spectral indices, including NDVI, SAVI, and burned area index (BAI) to distinguish burned land. They have demonstrated that BAI provided a better discrimination than the other tested indices, with a consistent behaviour along a considerable variability of scorched areas.

Table 3 sums up the presented indices, bands needed for their computation, formulas and references. Regarding the symbology, NIR, red, green, blue, SWIR are related with the spectral broadband and R_n stands for the reflectance value, in nanometres, on a certain narrowband. Broadband indices can also be computed with narrowband reflectance values from each spectral band. In thermal indices, there are different formulas that use temperature as T . There are also variables (e.g. L , G , a) representing parameterized features. Some authors use normalization schemes (Torres-Sánchez et al. 2014) as a pre-processing step before the use of values in the indices (e.g. green = green/red + green + blue; red = red/red + green + blue; blue = blue/red + green + blue).

4.3. Segmentation

Image processing techniques are frequently used as a complement to the VIs calculation. In this topic, segmentation is particularly important for agroforestry, agriculture and related areas inasmuch as it is responsible for the simplification of imagery data into subsets that enable an easier analysis regarding features of interest. Thresholding is a common segmentation method that can be applied to mask certain features and/or to highlight the desired information. Within this category, there is a noteworthy algorithm

that relies in the Otsu's method (Otsu 1979) and which can be applied to obtain two classes of pixels (e.g. to distinguish bare soil from vegetation). Summing up, this method calculates an optimal threshold requiring low computational costs.

Meyer and Neto (2008) used VI to determine a colour VI with an automatic threshold and to determine their accuracy using plant-soil-residue images. They compared the ExG, ExG–ExR, and NDV indices results with manual plant pixel extraction after applying Otsu's method. Among the tested indices, the ExG–ExR allows reaching the best results in the successful discrimination of plants from the bare soil.

Regarding early season vegetation detection, Torres-Sánchez, López-Granados, and Peña (2015) used two image acquisition sensors (RGB and multispectral) in three different types of crops: maize; sunflower, and wheat. The developed algorithm for object based image analysis (OBIA) was based on a multiresolution segmentation algorithm while the Otsu's method was applied for thresholding two VIs, more specifically ExG and NDVI.

Another used method is the watershed transform: a gradient magnitude-based method that consists in finding the pixels with the highest gradient intensity corresponding to region boundaries. It was successfully applied in the extraction of canopy from palm orchards (Cohen et al. 2005). Baluja et al. (2012) used watershed algorithm combined with NDVI image to identify rows in vineyard crops.

OBIA (Blaschke 2010) relies in the reduction of intra-class spectral variability caused by crown textures, gaps and shadows. First, a group of spatially adjacent pixels is aggregated into spectrally homogeneous features which are then classified using objects as the minimum processing units (Torres-Sánchez, López-Granados, and Peña 2015). OBIA was used to identify different types of plant canopy, in pure olive crowns detection (Calderón et al. 2013), in discontinuous and continuous olive orchards (Díaz-Varela et al. 2015) and also for weed map generation in maize fields (Peña et al. 2013).

In order to successfully detect vine rows using UAS imagery, Comba et al. (2015) used Hough Space Clustering and total least square. Their method can be applied to different types of images resulting from VI calculation (e.g. NDVI) or in a simple grayscale image, based on a single-band (e.g. NIR). Nolan et al. (2015) used skeletisation techniques to accurately segment vineyard rows to produce precise vine maps. The proposed algorithm uses as inputs single-band images from any type of sensor with the only requirement of having a high spatial resolution to distinguish vine rows and soil. The application of such an algorithm allowed Nolan et al. (2015) to achieve an accuracy of 97.1% regarding the identification of vineyard rows. The 2.9% failure rate occurred because of trees obscuring vine rows, shadows and also segmentation discontinuities. Bobillet et al. (2003) also classified vine rows; however, their method required manual adjustments in pre and post-processing stages to the achievement of valid results. Moreover, problems identifying vine rows with grass in between were reported.

4.4. 3D reconstruction

In agroforestry applications, vegetation can be accurately virtualized using 3D scanning methods. One of the most known of these methods involves the extraction of a point cloud from ground, crops and other field elements. As it was previously mentioned, lidar

can be used for 3D scanning. For example, Wallace (2013) used this sensor to digitalize forest's canopy.

Another known technique is the SfM, which provides the ability to create 3D models from 2D images. DSMs and crop surface models (CSMs) can be achieved using this technique. In turn, these models can be used to obtain important data regarding the elevation models and in crop development (Flener et al. 2013). The reconstruction process consists in the following steps: (1) matching the overlapping images containing the similar features; (2) extraction of geometry; (3) point cloud processing; and (4) 3D model and texture generation accordingly with the provided images. The main constraint of this method is the high demand of computational requirements and, consequently, the processing time. Bendig et al. (2014) conducted a study to monitor barley crops using the post-flight generated CSM computed by images acquired from a RGB camera mounted on a UAV. The study introduced a method to estimate biomass based on the plant height derived from CSM, demonstrating that RGB images are highly suitable for deriving barley plant height. Mathews and Jensen (2013) opted by applying SfM to compute a point cloud of vine canopy structure to estimate LAI. Figure 17 shows an example of a DSM obtained from 2D nadir images. Gatzliolis et al. (2015) used a multi-rotor UAV to capture images and achieve 3D reconstructions of trees with SfM algorithms. SfM techniques are becoming increasingly used due to their cost-effectiveness in comparison with expensive systems such as lidar. More recently, Thiel and Schmulius (2016) compared point clouds from UAV images with those created from lidar systems over a forested area and showed that the photogrammetric accuracy compares well with lidar, yet the density of surface points is much higher from images, which is of particular importance for the detection of small trees. Alternatively, there are other valid techniques for 3D reconstruction that are getting increasingly accessible, like the ones based on stereo cameras (Frankenberger, Huang, and Nouwakpo 2008; Honkavaara et al. 2013).

Wallace et al. (2016) carried out a comparison of airborne lidar scanning and SfM. Both methods proved to be capable of providing useful information about canopy and terrain in areas with low canopy closure. However, lidar outperformed SfM in capturing terrain under denser canopy cover. Díaz-Varela et al. (2015) worked with SfM-based



Figure 17. Digital surface model (DSM) of a UTAD's vineyard determined in the post-processing stage of a flight with an UAV carrying an optical sensor.

DSMs to estimate olive crown parameters such as tree height and crown diameter, in continuous and discontinuous canopy cropping systems. The estimation of crown parameters presented a high compliance with the real measurements.

Different applications are provided in the next section depending on the application area: agriculture, forestry, or both.

5. Applications

UAS provide high-resolution aerial imagery opening new cost-effective horizons that are capable of tackling the traditional and expansive remote-sensing platforms such as manned aircraft or satellites. In this section, some of the works that constitute the state of the art on applications relying on UAS will be reviewed to provide a better insight of the potential of these unmanned flight devices in agriculture, forestry and related areas, as presented in Table 4. In agriculture, the main applications include crop monitoring, invasive weed mapping, water status estimation, biomass estimation, chlorophyll estimation and nitrogen estimation. For forestry applications, bellow forest canopy mapping, forest inventory, measuring and monitoring structural forest properties, and forest fire detection and monitoring have been explored by the use of UAS. There are also applications common to both areas such as land-use classification, wildlife detection, and vegetation height maps.

5.1. Agriculture

UAS-based remote sensing can help determining plant parameters such as LAI, canopy cover and volume. UAVs provide flexibility to assess crop parameters as vigour, quality,

Table 4. UAS-based remote-sensing applications on agriculture, forestry and common to both areas.

Application	Main objective	References
Agriculture	Crop monitoring	Ballesteros et al. (2015), Berni et al. (2009), Calderón, Navas-Cortés, and Zarco-Tejada (2015), Candiago et al. (2015), Comba et al. (2015), Díaz-Varela et al. (2015), Kalisperakis et al. (2015), Lukas et al. (2016), Navia et al. (2016), Nebiker et al. (2008), Primicerio et al. (2012), Suomalainen et al. (2014), Torres-Sánchez, López-Granados, and Peña (2015), Torres-Sánchez et al. (2014), Turner, Lucieer, and Watson (2011)
	Invasive weed mapping	Gómez-Candón, Castro, and López-Granados (2013), Peña et al. (2013)
	Water status estimation	Baluja et al. (2012), Bellvert and Girona (2012), Bellvert et al. (2013), Park et al. (2015), Zarco-Tejada, González-Dugo, and Berni (2012)
	Biomass estimation	Bendig et al. (2014, Bendig 2015, Honkavaara et al., 2012, Honkavaara et al. (2013), Pölonen et al. (2013)
	Chlorophyll estimation	Uto et al. (2013), Zarco-Tejada, González-Dugo, and Berni (2012)
Forestry	Nitrogen estimation	Caturegli et al. (2016), Pölonen et al. (2013)
	Bellow forest canopy mapping	Chisholm et al. (2013), Getzin, Wiegand, and Schöning (2012)
	Forest inventory	Rokhmana (2015), Wallace et al. (2012)
	Measuring and monitoring structural forest properties	Gatzliolis et al. (2015), Wallace (2013), Wallace et al. (2016)
Agriculture and forestry	Forest fire detection and monitoring	Merino et al. (2011)
	Land-use classification	Lagüela et al. (2015)
	Wildlife detection	Israel (2011), Ward et al. (2016)
	Vegetation height maps	Ballesteros et al. (2015), Bendig et al. (2015), Mathews and Jensen (2013), Suomalainen et al. (2014), Turner, Lucieer, and Watson (2011)

and yield estimation, which is needed to be measured during the whole growing season, as presented in Ballesteros et al. (2015). For parameters that are hard to detect with visible spectrum sensors, hyperspectral sensors are more suitable. These sensors enable the acquisition of imagery data with very high spectral and temporal resolutions, which is especially adequate for disease detection in early stages (Calderón, Navas-Cortés, and Zarco-Tejada 2015) or precision agriculture (Candiago et al. 2015), reducing future losses. Farmers' interests are to have healthier crops and, at a same time, to manage resources (e.g. water and pesticides) in an efficient way. This can be provided by UAVs data to create maps for better crop management (Ballesteros et al. 2015). These maps are adequate to expose problems as irrigation, soil variation, fungal or pest investigation.

Usually, NIR sensors are not used separately, but in combination with RGB sensors or as a component in multispectral sensors. Navia et al. (2016) used multispectral imagery acquired from a multi-rotor UAV to generate multispectral mosaics computed with NDVI, to assist farmers in the assessment of plant health monitoring. Lukas et al. (2016) compared the basic growth parameters obtained from a fixed-wing UAV equipped with a NIR camera and from Landsat 8. Both methods showed a high correlation with ground spectrometer measurements of biomass and nitrogen content but the satellite data had a coarse resolution. Kalisperakis et al. (2015) used different UAS imaging sources, more specifically, hyperspectral, RGB orthophotographs and 3D crop surface models to access LAI estimation in vineyards. The comparison between estimated LAI and ground truth LAI measurements showed that the lowest correlation rates occurred from RGB orthophotographs. On the other hand, the highest correlation was noticed in hyperspectral data and 3D crop surface models.

Another application area in agriculture is invasive weed mapping. A study to distinguish the invasive weeds from other crops was carried out by Peña et al. (2013). It consisted on detecting weed in early stages of maize using a six band multispectral camera attached to an UAV in which the applied OBIA procedure computed multiple results and statistics that could be exported in the form of weed maps, vectors or table file format and provide relevant information. Another study to distinguish crops from invasive weed was carried out by Gómez-Candón, Castro, and López-Granados (2013) in wheat.

Water status estimation is a task that can be performed by UAVs with quick turn-around times. Bellvert et al. (2013) demonstrated the feasibility of using high-resolution thermal imagery for irrigation management across vineyards for precision agriculture purposes (optimal irrigation). According to Bellvert et al. (2013) the best time of the day to acquire thermal images is around noon, because there is an almost complete absence of shadow effects and, consequently, the sensitiveness for the identification of water stress problems is higher. Multispectral and thermal imagery was applied by Baluja et al. (2012) and Bellvert and Girona (2012) to determine water status variability in vineyards. This data can be used for better irrigation management in a vineyard parcel scale. Zarco-Tejada, González-Dugo, and Berni (2012) addressed the detection of water stress in a citrus orchard by using fluorescence, canopy temperature, and narrow-band indices, from data acquired by a micro-hyperspectral and a thermal camera.

Biomass estimation was studied by Bendig et al. (2014) with VIs and plant height maps derived from RGB imagery on barley. Three VIs were computed, with the main issue of the visible band being reliable only in early growing stages. However,

combining the VIs with plant height by using multiple linear regression or nonlinear regression models, a better performance was achieved, in comparison with the indices itself.

Chlorophyll estimation was addressed in the study carried out by Uto et al. (2013) focusing on the estimation of rice chlorophyll density, based on low altitude flights carried out by an UAV equipped with a hyperspectral sensor. Experimental results showed that the chlorophyll density can be estimated with high accuracy, even under unstable light conditions. Suomalainen et al. (2014) developed a hyperspectral sensor based on low-cost components, to apply it on multiple types of crops. Chlorophyll concentration was examined using red edge-based indices. Martín et al. (2015) used hyperspectral sensing to investigate the relation between leaves chlorophyll $a + b$ concentration and grapes composition in vineyards affected by iron chlorosis and to assess if the leaves chlorophyll concentration acquired from hyperspectral images could be useful to map potential quality zones in these vineyards. The results suggest a promising application for predicting grapes' quality in vineyards affected by the iron chlorosis.

Caturegli et al. (2016) focused on the estimation of nitrogen status in turfgrass. This kind of knowledge can lead to both economic and environmental benefits inasmuch as it enables the balanced application of fertilizers. In addition, pesticides are extensively applied for eliminating pests and weeds infesting the crops. Pölönen et al. (2013) were able to estimate both biomass and nitrogen content with a hyperspectral sensor and a machine learning approach.

5.2. Forestry

Getzin, Wiegand, and Schöning (2012) used a fixed-wing UAV to take aerial images of a forest aiming the further examination of canopy gaps and the assessment of the floristic biodiversity existent in the forest understorey. The obtained images led the authors to conclude that detailed spatially implicit information on gap shape metrics is sufficient to reveal strong dependency between disturbance patterns and plant diversity. Chisholm et al. (2013) conducted a trial with a lidar mounted on an UAV for mapping the forest below the canopy. The main goals were to map tree stems and to measure the diameter of trees at breast height (DBH). The lidar along with a developed algorithm enabled the detection of trees in flights of 3 m that took place 20 cm above the DBH.

To calculate wood stock of a teak wood forest in Indonesia, Rokhmana (2015) used orthophotograph mosaics and 3D models. The main prerequisite for this task was to distinguish individual trees so its height could be measured as well as the canopy diameter. As it was previously mentioned in Section 4.4, lidar is a good tool for the accurate extraction of 3D data. The comparison between tree canopy mapping and photogrammetric SfM was already addressed in the work of Wallace et al. (2012), showing that lidar outperforms SfM in bellow canopy mapping.

Gatzliolis et al. (2015) were able to reconstruct 3D models using RGB cameras from UAV along with SfM algorithms. This methodology can be applied to individual or to a group of trees providing useful information related, with for instance tree growth among time.

Merino et al. (2011) developed an UAS for automatic forest fire monitoring and measurement. It was based on multiple UAVs and a central station. The main payload consisted in infrared and visual cameras which extract fire related features

5.3. Agroforestry

There are tasks that can be applied in both agriculture and forestry. The case of generation of thermographic mosaics and thermographic DSMs from thermal sensors attached on a low cost multi-rotor UAV were used (Lagüela et al. 2015). Although agroforestry was not the primary focus, the methodology can be extended to land-use classification and water management according to the thermal response of objects.

Industrialization of agriculture brought many benefits but also an increased danger for wild animals living in agroforestry areas. Israel (2011) presented a light weight infrared thermal sensor attached to an UAV, which is capable of preventing many fatalities among the roe deer fawn communities on meadows and pastures, caused by machines. Ward et al. (2016) took the concept even further and created a system that can autonomously detect animals, determine their coordinates and generate maps displaying their locations ahead of the user. They have proved the effectiveness of UAS over ground based techniques such as camera traps or surveys on foot.

Vegetation height maps can be applied in agriculture or forestry areas. Several studies were conducted making good use of this information for creation of crop surface models (Bendig et al. 2014; Mathews and Jensen 2013) or even to forest canopy cover (Wallace 2013).

5.4. Recommendations towards UAS platform selection

Table 5 presents budget estimations for the acquisition of an UAS according to the coverage area and the sensor type, which is influenced by the intended application. For large areas (greater than 50 ha) a fixed-wing UAV is recommended due to the ability of quicker area coverage; on the other hand, a multi-rotor UAV is more suitable for smaller area coverage. However, the usage of a fixed-wing UAV requires a large space to perform safe landing operations – at least an area of 20 m × 100 m (for linear landing) – which is a drawback of this type of UAV. A practical example is the Douro wine region in Portugal, where the vineyard layout disposed in slopes along the river Douro makes the landing task challenging due to the lack of secure areas to accomplish it. Complementary to Table 5, Figure 18 illustrates the process of selecting the most appropriate UAS and sensors for the required task.

Essentially, rotor-based UAS are used to cover small areas whereas the fixed-wing UASs are more suitable for being applied in wider areas, as detailed in Table 5. On the other hand, the use of sensors is highly dependent of the application's purpose.

On the subject of forestry applications such as inventory and canopy mapping, the usage of lidar sensors represents an effective tool capable of gathering data below canopy. When it comes to perform forest fire monitoring and wildlife detection, thermal sensors are a suitable option, while for determining burned areas in post-fire scenario multi-spectral sensors can be applied.

Table 5. Recommended UAV platforms for different agroforestry applications and respective estimated budgets.

Area of application	Coverage area	Recommended sensor(s)	Recommended UAV	Estimated budget (Euros)
Crop monitoring	Large	Multispectral	Fixed-wing	25,000
	Small	Multispectral	Multi-rotor	10,000
Disease detection and identification	Large	Hyperspectral	Fixed-wing	120,000 ^a
	Small	Multispectral	Multi-rotor	10,000
Invasive weed mapping	Large	Multispectral	Fixed-wing	25,000
	Small	Multispectral	Multi-rotor	10,000
Water status estimation	Large	Thermal	Fixed-wing	35,000
	Small	Thermal	Multi-rotor	15,000
Biomass estimation	Large	Optical	Fixed-wing	20,000
	Small	Optical	Multi-rotor	2000
Chlorophyll estimation	Large	Hyperspectral	Fixed-wing	25,000
	Small	Hyperspectral	Multi-rotor	10,000
Bellow forest canopy mapping	Large	Lidar	Fixed-wing	30,000
Forest inventory	Large	Lidar	Fixed-wing	30,000
Measuring and monitoring structural forest properties	Large	Lidar	Fixed-wing	30,000
Forest fire detection and monitoring	Large	Thermal	Fixed-wing	35,000
Post-fire burn area estimation	Large	Multispectral	Fixed-wing	25,000
Wildlife detection	Small	Thermal	Multi-rotor	8000
Nitrogen estimation	Large	Multispectral	Fixed-wing	25,000
	Small	Multispectral	Multi-rotor	10,000
Vegetation height maps	Small	Optical	Multi-rotor	3000

Each UAV platform considers a UAV type (fixed-wing or multi-rotor) and an attachable sensor (optical, multispectral, hyperspectral, thermal, and lidar). Small areas up to 50 ha; Large areas between 50 ha and 5 km². The estimated budget includes UAV + sensor + processing software.

^aThe prices have been decreasing.

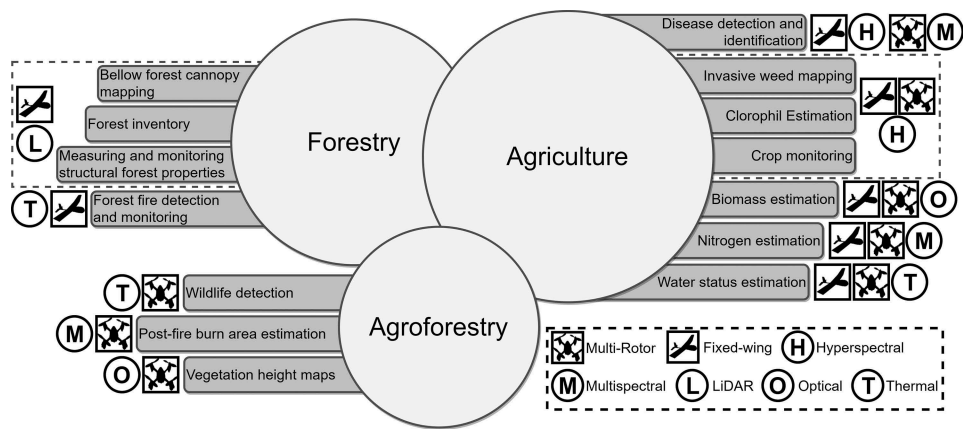


Figure 18. Diagram depicting an appropriate selection of a UAS platform – including UAV and sensor – depending on the area of application and the task.

To obtain vegetation height maps, optical sensors are a plausible choice, because of their ability to process the acquired images using SfM algorithms and the cost-effectiveness comparatively to sensors such as lidar. Crop monitoring along the whole growth season can be performed through multispectral sensors which seem to present the most compromise between cost and effectiveness. In spite of it, other sensors can

also be applied to do crop monitoring related tasks. For those who are interested in biomass estimation, optical sensors might be a good choice. Multispectral sensors can be applied to map invasive weeds and nitrogen estimation. While the first results from post-flight image processing algorithms (e.g. OBIA), the latter is by providing fertilization maps.

Disease detection and identification have a significant importance in agricultural applications, either for resource optimization and/or timely actions for preventive purposes. Thus and notwithstanding the costs, hyperspectral sensors are recommended even for early stage disease detection. Alternatively, depending on the crop type and disease, multispectral sensors can be used. Hyperspectral sensors are also suitable for chlorophyll estimation through narrow-band VI calculation on the acquired data, accordingly to the addressed studies.

Finally, water status can be estimated through a set of spectral VI that are calculated to determine vigour, based on data acquired from multispectral or optical sensors, yet thermal sensors can provide this type of data in a faster way, although some cautions concerning daytime must be taken due to effects of shadows, according to Bellvert et al. (2013). Thereby, it is recommended to use these sensors when the sun heading is at, approximately, 180° (solar noon).

Table 6, provides an overview of the reviewed studies regarding the main objective and conclusions, along with the used UAV types and the used sensors. It is noteworthy that fixed-wing UAVs are widely applied to land-use classification, water assessment, or even to provide data towards the optimization of agricultural tasks (e.g. crop management and pesticide administration) through the use of optical, thermal, multi, and hyperspectral sensors. Most of the reviewed studies preferred multi-rotor UAVs that can vary the specified set of sensors to perform fire monitoring, canopy development assessment, detection of vineyard rows, etc., and also because they are usually cheaper and more flexible for demonstrative/scientific studies. Notwithstanding the great number of successful approaches, there is an important aspect that should be retained: the specifications of each platform (in terms of area covering, flight time durability, payload capacity) should be attended along with the recommendations left on this article inasmuch as they intend to represent general guidelines to prevent unnecessary costs for mission accomplishment or potential failure in performing the required surveys in demanding situations. In the way that a fixed-wing UAV for water status assessment in a small crop area could be exaggerated, a regular rotor-based UAV could be time-consuming at monitoring biodiversity in an extensive forestry area due to the lower autonomy in terms of flight time.

Regarding UAV sensors, while the RGB sensors are suitable to find features within a certain area (e.g. vineyard rows detection, tree crown size estimation), to estimate LAI for green vegetation and invasive weed mapping. The infrared, multispectral, and hyperspectral sensors are specialized in identifying the presence/absence of certain components or materials (e.g. disease detection, water status estimation) within a scene through reflectance analysis and processing at certain wavebands that can range out of the visible spectrum. Lidar sensors can provide accurate measurements through laser pulses targeting land objects (e.g. vegetation height determination). The cost/task-effectiveness binomial has a relevant role when it comes to select a tool for data extraction. If the precision on estimating the presence of a certain feature in the

Table 6. Compilation of the reviewed studies presenting their respective main objectives and conclusions and UAV type and sensors used in each case.

Reference	Objective	Main conclusion	UAV type		Used sensors					
			FW	RB	O	T	M	H	L	
Lagüela et al. (2015)	Land-use classification	Successful land-use classification (buildings, tall vegetation, short vegetation)		•		•				
Primicerio et al. (2012)	Producing of vigour maps of vineyards based on NDVI	Results highly correlated with ground truth spectrometer		•				•		
Getzin, Wiegand, and Schöning (2012)	Use canopy gaps in forests to assess floristic biodiversity of the forest understory	High-resolution imagery can effectively assess biodiversity in temperate forests	•		•					
Gómez-Candón, Castro, and López-Granados (2013)	Assess the parameters that affect the accuracy of orthomosaics. Early weed mapping in wheat	Different altitude intervals did not show large differences in accuracy in generation of orthomosaics between 30 and 100 m.		•	•					
Baluja et al. (2012)	Assessment of water status variability in vineyards	Both multispectral and thermal methods were successful	•				•	•		
Israel (2011)	Detection of roe fawn deer on meadows	Field campaigns confirmed reliable real-time manual fawn deer detection		•		•				
Ward et al. (2016)	Detection of animals and displaying their location on a map	Successfully tested and development of a smartphone app integrated with the system		•		•				
Bendig et al. (2014)	Barley biomass monitoring by combining plant height and VIs	Optical images were highly suitable for deriving barley plant height from CSM for biomass estimation		•	•					
Turner, Lucieer, and Watson (2011)	Vineyard mapping	UAVs provide flexible on-demand multiple sensor data for the whole growing season and especially for the critical times with high spatial resolution		•	•	•	•			
Candiago et al. (2015)	Evaluation of multiple VI for precision agriculture applications	The VI were computed based on pixel values and delivered mainly qualitative results		•			•			
Honkavaara et al. (2012)	Combination of hyperspectral imagery and point clouds for biomass estimation	Successful implementation of the use of hyperspectral reflectance mosaics with point clouds for biomass estimation		•	•				•	
Uto et al. (2013)	Development of a low-cost light hyperspectral sensor for chlorophyll estimation in rice paddies	Experimental results proved that chlorophyll densities can be estimated with high accuracy		•					•	
Ballesteros et al. (2015)	Leaf area index, green canopy cover, and volume characterization of vineyards	The developed work could be useful in decision support to improve crop management, and optimize usage of pesticides and fertilizer	•		•					
Lukas et al. (2016)	Comparison of basic growth parameters of winter wheat obtained from UAV and satellite	Both methods showed a strong correlation with ground spectrometer measurements but satellite imagery provided a smaller resolution	•					•		

(Continued)

Table 6. (Continued).

			UAV type		Used sensors					
Reference	Objective	Main conclusion	FW	RB	O	T	M	H	L	
Comba et al. (2015)	Vineyard row detection	Successful detection of wine rows in grey-scale images obtained from a multispectral sensor		●				●		
Nebiker et al. (2008)	Producing of vigour maps of vineyards	Results highly correlated with ground truth classification		●	●			●		
Peña et al. (2013)	Weed mapping in maize	The algorithm efficiently identified crop rows, inner row weeds were successfully detected		●				●		
Caturegli et al. (2016)	Nitrogen status estimation in turfgrass	The knowledge of the nitrogen status can lead to both economic and environmental benefits by a reasonable application of fertilizers		●	●			●		
Navia et al. (2016)	Multispectral orthomosaic generation and NDVI calculation	Calculated NDVI showed that it can determine weak spots in crop areas and also see change in plant health over time		●				●		
Rokhmana (2015)	Teak wood forest stock estimation	Successful wood stock estimation	●		●					
Pölönen et al. (2013)	Biomass and nitrogen content estimation of wheat and barley	Results showed that the radiometric uniformity amongst individual images forming the image mosaics had impact the biomass estimation quality		●					●	
Suomalainen et al. (2014)	Development of an hyperspectral sensor and evaluation on various types of crops for orthomosaics and vegetation height maps	A lightweight hyperspectral mapping system was developed specifically for rotor-based UAV and presented the potential for agricultural mapping and monitoring applications		●					●	
Chisholm et al. (2013)	Bellow forest canopy mapping	The UAV-measured DBH estimates were strongly correlated with the human-based ones		●					●	
Wallace et al. (2012)	Development of a low-cost UAV Lidar sensor applied in forest inventory applications	Comparing with lidar sensors used in other remote-sensing platforms UAV-borne lidar produced point clouds with only slightly worse accuracies but with much higher point densities		●					●	
Wallace et al. (2016)	Measuring and monitoring structural properties of forests with airborne laser scanner and SfM techniques	Airborne laser scanner got better results in penetrating the upper canopy and vertical distribution of vegetation. SfM lacked the ability to penetrate dense canopy parts, which resulted in a poor definition of the mid and under-store		●	●				●	
Bendig et al. (2015)	Estimating biomass in barley using VI and plant height information	Visible band indices showed a better ability to model biomass in early growth stages in comparison to late growth stages		●				●		

(Continued)

Table 6. (Continued).

Reference	Objective	Main conclusion	UAV type		Used sensors					
			FW	RB	O	T	M	H	L	
Zarco-Tejada, González-Dugo, and Berni (2012)	Water stress detection in citrus orchards using hyperspectral imager and thermal camera	The experiment enabled water stress detection assessment by using crown temperature, visible and NIR narrow-band indices and chlorophyll fluorescence	•			•		•		
Bellvert et al. (2013)	Generating maps using CWSI for precision irrigation management in vineyards	Demonstration of the viability of thermal imagery for detecting the level of water stress in vineyards	•			•	•			
Calderón, Navas-Cortés, and Zarco-Tejada (2015)	Automatic methods for early detection of plant diseases	The results demonstrated that the developed methods at orchard scale are validated for flights in large areas consisting of olive orchards with different characteristics	•			•		•		
Nolan et al. (2015)	Automated detection and segmentation of vine rows using high-resolution UAS imagery in a commercial vineyard	The vine row detection algorithm achieved average precision and sensitivity results. Some sections of vine rows have been falsely classified as being non-vine row pixels, due to overhanging trees, shadows or initial binary segmentation discontinuities	•		•					
Mathews and Jensen (2013)	Using SfM to model vine canopy structure	Measured LAI of vine canopy had good results with metrics	•					•		
Kalisperakis et al. (2015)	Estimating crop LAI using hyperspectral data, 2D RGB mosaic and 3D crop surface models	The lowest correlations against the ground truth data were derived from the calculated greenness levels from the 2D RGB orthomosaics. The highest correlation rates were established for the hyperspectral and the 3D canopy levels		•	•				•	
Wehrhan, Rauneker, and Sommer (2016)	Quantification of spatial patterns of fresh phytomass and its relation to carbon export of lucerne	Among different tested VI, the EVI got the highest correlation between ground-based measurements of fresh phytomass of lucerne	•					•		
Berni et al. (2009)	Vegetation monitoring through the use of thermal and multispectral sensors	The obtained results make this platform suitable for a number of applications including precision farming and irrigation scheduling		•		•	•			
Bellvert and Girona (2012)	Usage of multispectral and thermal images for irrigation scheduling in vineyards	It was demonstrated the viability of high-resolution thermal imagery for detecting the water stress level in grapevines	•			•				
Torres-Sánchez et al. (2014)	Early-season crop monitoring in wheat using VIs	The ExG index is most suitable to calculate early stages crops with accuracy and spatial and temporal consistency		•	•					

(Continued)

Table 6. (Continued).

Reference	Objective	Main conclusion	UAV type		Used sensors					
			FW	RB	O	T	M	H	L	
Torres-Sánchez, López-Granados, and Peña (2015)	Detection of vegetation in early-season herbaceous crops (maize, sunflower and wheat)	An automatic thresholding for vegetation classification was achieved based on OBIA algorithm. Demonstrating its ability to automatically select a threshold from grey-level histograms		•	•		•			
Park et al. (2015)	Estimation of crop water stress in a nectarine orchard	The mapping of spatial variability of nectarine water stress was proved to be effective and an optimal tool to help in irrigation management		•		•				
Wallace (2013)	Investigating the use of UAV-borne lidar systems as a platform to gain knowledge of the canopy structure within forested environments	UAV-lidar data is suitable for use in monitoring changes in the canopy structure. The method based on alpha shapes was the most stable across repeat measures		•						•
Gatzliolis et al. (2015)	Developing an affordable method for obtaining precise and comprehensive 3D models of trees and small groups of trees	The developed work proved to be capable of handling most conditions encountered in practice to deliver detailed reconstruction of trees		•	•					•
Honkavaara et al. (2013)	Investigating the processing and use of UAS image data in precision agriculture	Fundamental need to develop reliable methods for the geometric and radiometric processing of huge numbers of small, overlapping images as well as developing all-weather processing technology in order to take full advantage of this new technology and to make this technology operational in practical applications was identified		•						•
Díaz-Varela et al. (2015)	Estimating of olive crown parameters	Comparison between reference field measurements and remote-sensing estimation of crown parameters confirmed as a good solution in terms of performance and cost-effective alternative for the characterization of the olive tree crown in discontinuous canopy	•		•					
Mathews (2015)	The use of compact digital cameras to remotely estimate spectral reflectance based on UAV imagery	There was found that the red and NIR bands were the most accurate at estimating reflectance	•							•
Merino et al. (2011)	Automatic fire detection	A system for fire monitoring was developed, based on several UAVs and a central station. Infrared and visual cameras were the main payload used for the environment perception		•	•	•				

FW: fixed-wing; RB: rotor-based; O: optical; T: thermal; M: multispectral; H: hyperspectral; L: lidar.

environment (e.g. vineyard disease) is required, the use of a hyperspectral sensor should be considered. In an alternative scenario, when a low-budget system is required, for instance to produce 3D models of a certain culture for analysing different development stages, an RGB camera allied to photogrammetric techniques will be sufficient (despite the probable loss of information – e.g. soil – over the obvious, but usually expensive, lidar sensor).

6. Conclusion

This survey presents a brief comparison of remote-sensing platforms, their pros and cons, and how UASs can complement the established manned aircraft and satellite platforms. Most common types of UAVs and sensors are also presented aside with processing methods and applications in agroforestry. This study provides agroforestry professionals with information to assist them in choosing the most suitable UAS for their remote-sensing purposes. To achieve this, recent studies were reviewed with the focus on UAV types, sensors, data processing and applications in agroforestry.

Before selecting a proper UAS, the end-user should understand the capabilities and the restrictions of the available systems regarding not only the kind of results that are expected, but also what to do with them since mosaics, digital surface models, VIs, etc., are not the final products but resources for further goals. UAS-based remote sensing in precision farming and forestry aims to provide the adequate decision support, which has a crucial role for the management optimization of farms, woodlands and other similar territorial areas.

Nowadays, farmers and foresters are dependent on companies to perform the processing and presentation of agroforestry-related information, sometimes in a way that will not fulfil the end-user needs. The next step of this ongoing revolution will focus in the development of user-friendly interfaces where just a few parameters are required, releasing the user from a deeper knowledge on data processing, allowing agroforestry professionals to perform interpretation of collected data by UAS in an autonomous and easy way. Our research group is already developing effective solutions allowing the professionals an autonomous analysis.

Better data processing software working with different sources of temporal and spatial data (e.g. meteorological and environmental) for a more effective decision support regarding agroforestry applications will also appear in the near future. Ideally, the future of both precision agriculture and agroforestry remote sensing would be to have the UAVs platforms constantly sensing the environment and sending the resulting data to intelligent entities (centralized or distributed) that control actuators to optimally solve eventual issues such as the lack of water or disease detection in a complete solution of Internet of Things for agroforestry. This kind of proactivity would allow farmers and foresters to be concentrated on the final products and services instead of being concerned with the middle-level processes.

Summing up, UAS platforms with the addressed sensors are going mainstream and its importance for decision support is getting increasingly relevant for researchers, farmers, foresters, and related business professionals as innovative techniques are being developed for a sharpen optimization of the agroforestry underlying processes. DroneDeploy

(2016) use case statistics confirm that agriculture, including forestry, is the leading application in the UAS market and Simelli and Tsagaris (2015) refer that by 2018, the usage of UAS will continue to grow with increasing affordability and autonomy. In spite of the fact that the UAV can fly autonomously, nowadays it is still required the presence of a pilot. The reasons of this are the lack of device intelligence. Hopefully, this issue will be solved in the next years due to the expansion of UAS usage in many sectors and mainly because of the progress of the artificial intelligence, which is capable of providing the autonomous decision support to those devices including law awareness. The optimal scenario of using UAVs is the entire automated process from taking off the vehicle to the processing the data and turning on the pro-active actions. In the agricultural industry, the UAV would do the flights in the area of interest whenever it would be needed, based on previous flights. The collected data would serve as information for other automated machines, such as irrigation systems or intelligent pesticide sprayers.

Acknowledgements

This work was financed by the European Regional Development Fund (ERDF) through the Operational Programme for Competitiveness and Internationalisation - COMPETE 2020 under the PORTUGAL 2020 Partnership Agreement, and through the Portuguese National Innovation Agency (ANI) as a part of project "PARRA - Plataforma integrAda de monitoRização e avaliação da doença da flavescência douRada na vinha" (Nº 3447) and ERDF and North 2020 – North Regional Operational Program, as part of project "INNOVINE&WINE – Vineyard and Wine Innovation Platform" (NORTE-01-0145-FEDER-000038).

Disclosure statement

No potential conflict of interest was reported by the authors.

Funding

This work was financed by the European Regional Development Fund (ERDF) through the Operational Programme for Competitiveness and Internationalisation - COMPETE 2020 under the PORTUGAL 2020 Partnership Agreement, and through the Portuguese National Innovation Agency (ANI) as a part of project "PARRA - Plataforma integrAda de monitoRização e avaliação da doença da flavescência douRada na vinha" (Nº 3447) and ERDF and North 2020 – North Regional Operational Program, as part of project "INNOVINE&WINE – Vineyard and Wine Innovation Platform" (NORTE-01-0145-FEDER-000038).

ORCID

Joaquim J. Sousa  <http://orcid.org/0000-0003-4533-930X>

References

- Ambrosia, V. G., S. Wegener, T. Zajkowski, D. V. Sullivan, S. Buechel, F. Enomoto, ... E. Hinkley. 2011. "The Ikhana Unmanned Airborne System (UAS) Western States Fire Imaging Missions: From

- Concept to Reality (2006–2010).” *Geocarto International* 26 (2): 85–101. doi:10.1080/10106049.2010.539302.
- Amon, P., U. Riegl, P. Rieger, and M. Pfennigbauer, & OTHERS. (2015). UAV-Based Laser Scanning to Meet Special Challenges in LiDAR Surveying. Retrieved from <http://www.ee.co.za/wp-content/uploads/2015/08/Philipp-Amon-Ursula-Riegl-Peter-Rieger-Martin-Pfennigbauer.pdf>
- Anderson, K., and K. J. Gaston. 2013. “Lightweight Unmanned Aerial Vehicles will Revolutionize Spatial Ecology.” *Frontiers in Ecology and the Environment* 11 (3): 138–146. doi:10.1890/120150.
- Austin, R. (2010). *Unmanned Aircraft Systems: UAVS Design, Development and Deployment* - Reg Austin. Retrieved July 8, 2016, from <http://eu.wiley.com/WileyCDA/WileyTitle/productCd-0470058196.html>
- AUVSI Economic Report, 2013. The Economic Impact of Unmanned Aircraft Systems Integration in the United States. Available online at: https://higherlogicdownload.s3.amazonaws.com/AUVSI/958c920a-7f9b-4ad2-9807-f9a4e95d1ef1/UploadedImages/New_Economic%20Report%202013%20Full.pdf (accessed 17 January 2017).
- Ballesteros, R., J. F. Ortega, D. Hernández, and M. Á. Moreno. 2015. “Characterization of Vitis vinifera L. Canopy Using Unmanned Aerial Vehicle-Based Remote Sensing and Photogrammetry Techniques.” *American Journal of Enology and Viticulture*, ajev.2014.14070. 10.5344/ajev.2014.14070.
- Baluja, J., M. P. Diago, P. Balda, R. Zorer, F. Meggio, F. Morales, and J. Tardaguila. 2012. “Assessment of Vineyard Water Status Variability by Thermal And Multispectral Imagery Using an Unmanned Aerial Vehicle (UAV).” *Irrigation Science* 30 (6): 511–522. doi:10.1007/s00271-012-0382-9.
- Bareth, G., J. Bendig, N. Tilly, D. Hoffmeister, H. Aasen, and A. Bolten. 2016. “A Comparison of UAV- and TLS-derived Plant Height for Crop Monitoring: Using Polygon Grids for the Analysis of Crop Surface Models (CSMs).” *Photogrammetrie - Fernerkundung - Geoinformation* 2016 (2): 85–94. doi:10.1127/pfg/2016/0289.
- Bellvert, J., and J. Girona. 2012. “The Use of Multispectral and Thermal Images as a Tool for Irrigation Scheduling in Vineyards.” In *The Use of Remote Sensing and Geographic Information Systems for Irrigation Management in Southwest Europe*, eds M. Erena, A. López-Francos, S. Montesinos, and J. F. Y Berthoumieu, 131–138, Zaragoza: Options Méditerranéennes. Serie B: Studies and Researchs, (67).
- Bellvert, J., J. Marsal, J. Girona, V. Gonzalez-Dugo, E. Fereres, S. L. Ustin, and P. J. Zarco-Tejada. 2016. “Airborne Thermal Imagery to Detect the Seasonal Evolution of Crop Water Status in Peach, Nectarine and Saturn Peach Orchards.” *Remote Sensing* 8 (1): 39. doi:10.3390/rs8010039.
- Bellvert, J., P. J. Zarco-Tejada, J. Girona, and E. Fereres. 2013. “Mapping Crop Water Stress Index in a “Pinot-noir” Vineyard: Comparing Ground Measurements with Thermal Remote Sensing Imagery from an Unmanned Aerial Vehicle.” *Precision Agriculture* 15 (4): 361–376. doi:10.1007/s11119-013-9334-5.
- Bendig, J., A. Bolten, S. Bennertz, J. Broscheit, S. Eichfuss, and G. Bareth. 2014. “Estimating Biomass of Barley Using Crop Surface Models (CSMs) Derived from UAV-Based RGB Imaging.” *Remote Sensing* 6 (11): 10395–10412. doi:10.3390/rs61110395.
- Bendig, J., K. Yu, H. Aasen, A. Bolten, S. Bennertz, J. Broscheit, . . . G. Bareth. 2015. “Combining UAV-Based Plant Height from Crop Surface Models, Visible, and Near Infrared Vegetation Indices for Biomass Monitoring in Barley.” *International Journal of Applied Earth Observation and Geoinformation* 39: 79–87. doi:10.1016/j.jag.2015.02.012.
- Bendig, J. V. 2015. *Unmanned Aerial Vehicles (UAVs) for Multi-Temporal Crop Surface Modelling. A New Method for Plant Height and Biomass Estimation Based on RGB-Imaging*. Cologne: Universität zu Köln. Retrieved from: <http://kups.ub.uni-koeln.de/6018/>.
- Berni, J. A. J., P. J. Zarco-Tejada, L. Suarez, and E. Fereres. 2009. “Thermal and Narrowband Multispectral Remote Sensing for Vegetation Monitoring from an Unmanned Aerial Vehicle.” *IEEE Transactions on Geoscience and Remote Sensing* 47 (3): 722–738. doi:10.1109/TGRS.2008.2010457.
- Blaschke, T. 2010. “Object Based Image Analysis for Remote Sensing.” *ISPRS Journal of Photogrammetry and Remote Sensing* 65 (1): 2–16. doi:10.1016/j.isprsjrs.2009.06.004.

- Bobillet, W., J. P. Da Costa, C. Germain, O. Laviolle, and G. Grenier (2003). Row Detection in High Resolution Remote Sensing Images of Vine Fields. In *Precision Agriculture: Papers from the 4th European Conference on Precision Agriculture* (pp. 81–87). Berlin, Germany.
- Bramley, R. G. V., and R. P. Hamilton. 2007. "Terroir and Precision Viticulture: Are They Compatible?" *Journal International Des Sciences de La Vigne et Du Vin* 41 (1): 1.
- Calderón, R., J. A. Navas-Cortés, C. Lucena, and P. J. Zarco-Tejada. 2013. "High-resolution Airborne Hyperspectral and Thermal Imagery for Early Detection of Verticillium Wilt of Olive Using Fluorescence, Temperature and Narrow-Band Spectral Indices. ." *Remote Sensing of Environment* 139: 231–245. doi:10.1016/j.rse.2013.07.031.
- Calderón, R., J. A. Navas-Cortés, and P. J. Zarco-Tejada. 2015. "Early Detection and Quantification of Verticillium Wilt in Olive Using Hyperspectral and Thermal Imagery over Large Areas." *Remote Sensing* 7 (5): 5584–5610. doi:10.3390/rs70505584.
- Candiago, S., F. Remondino, M. De Giglio, M. Dubbini, and M. Gattelli. 2015. "Evaluating Multispectral Images and Vegetation Indices for Precision Farming Applications from UAV Images." *Remote Sensing* 7 (4): 4026–4047. doi:10.3390/rs70404026.
- Caturegli, L., M. Corniglia, M. Gaetani, N. Grossi, S. Magni, M. Migliazzi, ... M. Volterrani. 2016. "Unmanned Aerial Vehicle to Estimate Nitrogen Status of Turfgrasses." *PLoS One* 11 (6): e0158268. doi:10.1371/journal.pone.0158268.
- Chisholm, R. A., J. Cui, S. K. Y. Lum, and B. M. Chen. 2013. "UAV LiDAR for Below-Canopy Forest Surveys." *Journal of Unmanned Vehicle Systems* 1 (1): 61–68. doi:10.1139/juvs-2013-0017.
- Chuvieco, E., M. P. Martín, and A. Palacios. 2002. "Assessment of Different Spectral Indices in the Red-Near-Infrared Spectral Domain for Burned Land Discrimination." *International Journal of Remote Sensing* 23 (23): 5103–5110. doi:10.1080/01431160210153129.
- Cohen, Y., V. Alchanatis, M. Meron, Y. Saranga, and J. Tsipris. 2005. "Estimation of Leaf Water Potential by Thermal Imagery and Spatial Analysis." *Journal of Experimental Botany* 56 (417): 1843–1852. doi:10.1093/jxb/eri174.
- Colomina, I., and P. Molina. 2014. "Unmanned Aerial Systems For Photogrammetry and Remote Sensing: A Review." *ISPRS Journal of Photogrammetry and Remote Sensing* 92: 79–97. doi:10.1016/j.isprsjprs.2014.02.013.
- Comba, L., P. Gay, J. Primicerio, and D. Ricauda Aimonino. 2015. "Vineyard Detection from Unmanned Aerial Systems Images." *Computers and Electronics in Agriculture* 114: 78–87. doi:10.1016/j.compag.2015.03.011.
- Cracknell, A. P. 2017. "xxx." *International Journal of Remote Sensing* 38: yyyy–zzzz.
- DroneDeploy (2016). *Commercial Drone Industry Trends*. DroneDeploy's Commercial Drone Industry Trends. Retrieved from <http://info.dronedeploy.com/commercial-drone-industry-trends/>.
- Díaz-Varela, R. A., R. De La Rosa, L. León, and P. J. Zarco-Tejada. 2015. "High-Resolution Airborne UAV Imagery to Assess Olive Tree Crown Parameters Using 3D Photo Reconstruction: Application in Breeding Trials." *Remote Sensing* 7 (4): 4213–4232. doi:10.3390/rs70404213.
- Falkowski, M. J., P. E. Gessler, P. Morgan, A. T. Hudak, and A. M. S. Smith.; (2005). *Characterizing and Mapping Forest Fire Fuels Using ASTER Imagery And Gradient Modeling*. Retrieved from <http://www.treesearch.fs.fed.us/pubs/23874> 10.1016/j.foreco.2005.06.013
- Flener, C., M. Vaaja, A. Jaakkola, A. Krooks, H. Kaartinen, A. Kukko, ... P. Alho. 2013. "Seamless Mapping of River Channels at High Resolution Using Mobile LiDAR and UAV-Photography." *Remote Sensing* 5 (12): 6382–6407. doi:10.3390/rs5126382.
- Frankenberger, J. R., C. Huang, and K. Nouwakpo. 2008. "Low-Altitude Digital Photogrammetry Technique to Assess Ephemeral Gully Erosion." In *IGARSS 2008-2008 IEEE International Geoscience and Remote Sensing Symposium* 4: IV-117-IV-120. doi:10.1109/IGARSS.2008.4779670.
- Galiano, S. G. 2012. "Assessment of Vegetation Indexes from Remote Sensing: Theoretical Basis." *Paseo Alfonso XIII* 52: 65–75.
- Gamon, J. A., J. Peñuelas, and C. B. Field. 1992. "A Narrow-Waveband Spectral Index that Tracks Diurnal Changes In Photosynthetic Efficiency." *Remote Sensing of Environment* 41 (1): 35–44. doi:10.1016/0034-4257(92)90059-S.

- Gao, B. 1996. "NDWI—A Normalized Difference Water Index for Remote Sensing of Vegetation Liquid Water from Space." *Remote Sensing of Environment* 58 (3): 257–266. doi:[10.1016/S0034-4257\(96\)00067-3](https://doi.org/10.1016/S0034-4257(96)00067-3).
- García, M. J. L., and V. Caselles. 1991. "Mapping Burns and Natural Reforestation Using Thematic Mapper Data." *Geocarto International* 6 (1): 31–37. doi:[10.1080/10106049109354290](https://doi.org/10.1080/10106049109354290).
- Gatzliolis, D., J. F. Lienard, A. Vogs, and N. S. Strigul. 2015. "3D Tree Dimensionality Assessment Using Photogrammetry and Small Unmanned Aerial Vehicles." *PLoS One* 10 (9): e0137765. doi:[10.1371/journal.pone.0137765](https://doi.org/10.1371/journal.pone.0137765).
- Geipel, J., G. G. Peteinatos, W. Claupein, and R. Gerhards. 2013. "Enhancement of Micro Unmanned Aerial Vehicles for Agricultural Aerial Sensor Systems." In *Precision Agriculture '13*, Ed. J. V. Stafford, 161–167. Wageningen, The Netherlands: Wageningen Academic Publishers. doi:[10.3920/978-90-8686-778-3_18](https://doi.org/10.3920/978-90-8686-778-3_18).
- George, E. A., G. Tiwari, R. N. Yadav, E. Peters, and S. Sadana (2013). UAV Systems for Parameter Identification in Agriculture. In *Global Humanitarian Technology Conference: South Asia Satellite (GHTC-SAS)*, 2013 IEEE (pp. 270–273). Retrieved from http://ieeexplore.ieee.org/xpls/abs_all.jsp?arnumber=6629929
- Gertler, J. (2012). US Unmanned Aerial Systems. DTIC Document. Retrieved from <http://oai.dtic.mil/oai/oai?verb=getRecord&metadataPrefix=html&identifier=ADA566235>
- Getzin, S., K. Wiegand, and I. Schöning. 2012. "Assessing Biodiversity in Forests Using Very High-Resolution Images and Unmanned Aerial Vehicles." *Methods in Ecology and Evolution* 3 (2): 397–404. doi:[10.1111/j.2041-210X.2011.00158.x](https://doi.org/10.1111/j.2041-210X.2011.00158.x).
- Gitelson, A. A., Y. J. Kaufman, and M. N. Merzlyak. 1996. "Use of a Green Channel in Remote Sensing of Global Vegetation from EOS-MODIS." *Remote Sensing of Environment* 58 (3): 289–298. doi:[10.1016/S0034-4257\(96\)00072-7](https://doi.org/10.1016/S0034-4257(96)00072-7).
- Gitelson, A. A., Y. J. Kaufman, R. Stark, and D. Rundquist. 2002. "Novel Algorithms for Remote Estimation of Vegetation Fraction." *Remote Sensing of Environment* 80 (1): 76–87. doi:[10.1016/S0034-4257\(01\)00289-9](https://doi.org/10.1016/S0034-4257(01)00289-9).
- Gnyp, M. L., G. Bareth, F. Li, V. I. S. Lenz-Wiedemann, W. Koppe, Y. Miao, ... F. Zhang. 2014. "Development and Implementation of a Multiscale Biomass Model Using Hyperspectral Vegetation Indices for Winter Wheat in the North China Plain." *International Journal of Applied Earth Observation and Geoinformation* 33: 232–242. doi:[10.1016/j.jag.2014.05.006](https://doi.org/10.1016/j.jag.2014.05.006).
- Gómez-Candón, D., A. I. D. Castro, and F. López-Granados. 2013. "Assessing the Accuracy of Mosaics from Unmanned Aerial Vehicle (UAV) Imagery for Precision Agriculture Purposes in Wheat." *Precision Agriculture* 15 (1): 44–56. doi:[10.1007/s11119-013-9335-4](https://doi.org/10.1007/s11119-013-9335-4).
- Gonzalez-Dugo, V., P. Zarco-Tejada, E. Nicolás, P. A. Nortes, J. J. Alarcón, D. S. Intrigliolo, and E. Fereres. 2013. "Using High Resolution UAV Thermal Imagery to Assess the Variability in the Water Status of Five Fruit Tree Species within a Commercial Orchard." *Precision Agriculture* 14 (6): 660–678. doi:[10.1007/s11119-013-9322-9](https://doi.org/10.1007/s11119-013-9322-9).
- Grenzdörffer, G. J., A. Engel, and B. Teichert. 2008. "The Photogrammetric Potential of Low-Cost UAVs in Forestry and Agriculture." *The International Archives of the Photogrammetry, Remote Sensing and Spatial Information Sciences* 31 (B3): 1207–1214.
- Haboudane, D., J. R. Miller, N. Tremblay, P. J. Zarco-Tejada, and L. Dextraze. 2002. "Integrated Narrow-Band Vegetation Indices for Prediction of Crop Chlorophyll Content for Application to Precision Agriculture." *Remote Sensing of Environment* 81 (2–3): 416–426. doi:[10.1016/S0034-4257\(02\)00018-4](https://doi.org/10.1016/S0034-4257(02)00018-4).
- Hague, T., N. D. Tillett, and H. Wheeler. 2006. "Automated Crop and Weed Monitoring in Widely Spaced Cereals." *Precision Agriculture* 7 (1): 21–32. doi:[10.1007/s11119-005-6787-1](https://doi.org/10.1007/s11119-005-6787-1).
- Hardin, P. J., and R. R. Jensen. 2011. "Small-Scale Unmanned Aerial Vehicles in Environmental Remote Sensing: Challenges and Opportunities." *GIScience & Remote Sensing* 48 (1): 99–111. doi:[10.2747/1548-1603.48.1.99](https://doi.org/10.2747/1548-1603.48.1.99).
- Herwitz, S. R., L. F. Johnson, S. E. Dunagan, R. G. Higgins, D. V. Sullivan, J. Zheng, ... J. A. Brass. 2004. "Imaging from an Unmanned Aerial Vehicle: Agricultural Surveillance and Decision Support." *Computers and Electronics in Agriculture* 44 (1): 49–61. doi:[10.1016/j.compag.2004.02.006](https://doi.org/10.1016/j.compag.2004.02.006).

- Holden, Z. A., P. Morgan, A. M. S. Smith, M. G. Rollins, and P. E. Gessler. (2005). Evaluation of Novel Thermally Enhanced Spectral Indices for Mapping Fire Perimeters and Comparisons with Fire Atlas Data. Retrieved from <http://www.treesearch.fs.fed.us/pubs/24608> 10.1080/01431160500239008
- Honkavaara, E., J. Kaivosoja, J. Mäkynen, I. Pellikka, L. Pesonen, H. Saari, ... T. Rosnell. 2012. "Hyperspectral Reflectance Signatures and Point Clouds for Precision Agriculture by Light Weight UAV Imaging System." *ISPRS Annals of Photogrammetry, Remote Sensing and Spatial Information Sciences* 1-7: 353–358. doi:10.5194/isprsannals-i-7-353-2012.
- Honkavaara, E., H. Saari, J. Kaivosoja, I. Pölönen, T. Hakala, P. Litkey, ... L. Pesonen. 2013. "Processing and Assessment of Spectrometric, Stereoscopic Imagery Collected Using a Lightweight UAV Spectral Camera for Precision Agriculture." *Remote Sensing* 5 (10): 5006–5039. doi:10.3390/rs5105006.
- Huete, A. R. 1988. "A Soil-Adjusted Vegetation Index (SAVI)." *Remote Sensing of Environment* 25 (3): 295–309. doi:10.1016/0034-4257(88)90106-X.
- Idso, S. B., R. D. Jackson, P. J. Pinter, R. J. Reginato, and J. L. Hatfield. 1981. "Normalizing the Stress-Degree-Day Parameter for Environmental Variability." *Agricultural Meteorology* 24: 45–55. doi:10.1016/0002-1571(81)90032-7.
- Israel, M. 2011. "A UAV-Based Roe Deer Fawn Detection System." *International Archives of Photogrammetry and Remote Sensing* 38: 1–5.
- Jenkins, D., and B. Vasigh (2013, March). Economic Report of Unmanned Aircraft Systems Integration in the United States. Association for Unmanned Vehicle Systems International. Retrieved from <http://www.auvsi.org/auvsiresources/economicreport>
- Jenks, C. 2010. "Law from above: Unmanned Aerial Systems, Use of Force, and the Law of Armed Conflict." *North Dakota Law Review* 85: 649.
- Jia, Y., Z. Su, Q. Zhang, Y. Zhang, Y. Gu, and Z. Chen. 2015. "Research on UAV Remote Sensing Image Mosaic Method Based on SIFT." *International Journal of Signal Processing, Image Processing and Pattern Recognition* 8 (11): 365–374. doi:10.14257/ijsp.2015.8.11.33.
- Jones, H. G. 1999. "Use of Infrared Thermometry for Estimation of Stomatal Conductance as a Possible Aid to Irrigation Scheduling." *Agricultural and Forest Meteorology* 95 (3): 139–149. doi:10.1016/S0168-1923(99)00030-1.
- Jordan, C. F. 1969. "Derivation of Leaf-Area Index from Quality of Light on the Forest Floor." *Ecology* 50 (4): 663–666. doi:10.2307/1936256.
- Justice, C. O., E. Vermote, J. R. G. Townshend, R. Defries, D. P. Roy, D. K. Hall, ... M. J. Barnsley. 1998. "The Moderate Resolution Imaging Spectroradiometer (MODIS): Land Remote Sensing for Global Change Research." *IEEE Transactions on Geoscience and Remote Sensing* 36 (4): 1228–1249. doi:10.1109/36.701075.
- Juul, M. (2015, October). Civil Drones in the European Union - Think Tank. Retrieved July 19, 2016, from [http://www.europarl.europa.eu/thinktank/en/document.html?reference=EPRS_BRI\(2015\)571305](http://www.europarl.europa.eu/thinktank/en/document.html?reference=EPRS_BRI(2015)571305)
- Kalisperakis, I., C. Stentoumis, L. Grammatikopoulos, and K. Karantzalos. 2015. "Leaf Area Index Estimation in Vineyards from UAV Hyperspectral Data, 2D Image Mosaics and 3D Canopy Surface Models." *ISPRS - International Archives of the Photogrammetry, Remote Sensing and Spatial Information Sciences* XL-1/W4: 299–303. doi:10.5194/isprsarchives-XL-1-W4-299-2015.
- Klemas, V. V. 2015. "Coastal and Environmental Remote Sensing from Unmanned Aerial Vehicles: An Overview." *Journal of Coastal Research* 1260–1267. doi:10.2112/JCOASTRES-D-15-00005.1.
- Lagüela, S., L. Díaz-Vilariño, D. Roca, and H. Lorenzo. 2015. "Aerial Thermography from Low-Cost UAV for the Generation of Thermographic Digital Terrain Models." *Opto-Electronics Review* 23 (1): 78–84. doi:10.1515/oere-2015-0006.
- López-López, M., R. Calderón, V. González-Dugo, P. J. Zarco-Tejada, and E. Fereres. 2016. "Early Detection and Quantification of Almond Red Leaf Blotch Using High-Resolution Hyperspectral and Thermal Imagery." *Remote Sensing* 8 (4): 276. doi:10.3390/rs8040276.
- Lukas, V., J. Novák, L. Neudert, I. Svobodova, F. Rodriguez-Moreno, M. Edrees, and J. Kren. 2016. "The Combination of UAV Survey and Landsat Imagery for Monitoring of Crop Vigor in Precision

- Agriculture." ISPRS - International Archives of the Photogrammetry, Remote Sensing and Spatial Information Sciences XLI-B8: 953–957. doi:[10.5194/isprsarchives-XLI-B8-953-2016](https://doi.org/10.5194/isprsarchives-XLI-B8-953-2016).
- Malinowski, R., B. Höfle, K. Koenig, G. Groom, W. Schwanghart, and G. Heckrath. 2016. "Local-Scale Flood Mapping on Vegetated Floodplains from Radiometrically Calibrated Airborne LiDAR Data." *ISPRS Journal of Photogrammetry and Remote Sensing* 119: 267–279. doi:[10.1016/j.isprsjprs.2016.06.009](https://doi.org/10.1016/j.isprsjprs.2016.06.009).
- Martín Isabel, M., P. Del, and E. Chuvieco Salinero (1998). Cartografía de grandes incendios forestales en la Península Ibérica a partir de imágenes NOAA-AVHRR. Retrieved from <http://dspace.uah.es/dspace/handle/10017/1059>
- Martín, P., P. J. Zarco-Tejada, M. R. González, and A. Berjón. 2015. "Using Hyperspectral Remote Sensing to Map Grape Quality in "Tempranillo" Vineyards Affected by Iron Deficiency Chlorosis." *VITIS - Journal of Grapevine Research* 46 (1): 7.
- Mateo, A., P. Toscano, S. F. Di Gennaro, L. Genesio, F. P. Vaccari, J. Primicerio, ... B. Gioli. 2015. "Intercomparison of UAV, Aircraft and Satellite Remote Sensing Platforms for Precision Viticulture." *Remote Sensing* 7 (3): 2971–2990. doi:[10.3390/rs70302971](https://doi.org/10.3390/rs70302971).
- Mathews, A. J. 2015. "A Practical Uav Remote Sensing Methodology To Generate Multispectral Orthophotos For Vineyards: Estimation of Spectral Reflectance Using Compact Digital Cameras." *International Journal of Applied Geospatial Research* 6(4): 65–87. doi:[10.4018/ijagr.2015100104](https://doi.org/10.4018/ijagr.2015100104).
- Mathews, A. J., and J. L. R. Jensen. 2013. "Visualizing and Quantifying Vineyard Canopy LAI Using an Unmanned Aerial Vehicle (UAV) Collected High Density Structure from Motion Point Cloud." *Remote Sensing* 5 (5): 2164–2183. doi:[10.3390/rs5052164](https://doi.org/10.3390/rs5052164).
- Mejias, L., J. Lai, and T. Bruggemann. 2015. Sensors for Missions. In *Handbook of Unmanned Aerial Vehicles* (pp. 385–399), Eds. K. P. Valavanis and G. J. Vachtsevanos, Dordrecht, The Netherlands: Springer. Retrieved from: http://link.springer.com/10.1007/978-90-481-9707-1_6.
- Merino, L., F. Caballero, J. R. Martínez-De-Dios, I. Maza, and A. Ollero. 2011. "An Unmanned Aircraft System for Automatic Forest Fire Monitoring and Measurement." *Journal of Intelligent & Robotic Systems* 65 (1–4): 533–548. doi:[10.1007/s10846-011-9560-x](https://doi.org/10.1007/s10846-011-9560-x).
- Meyer, G. E., and J. C. Neto. 2008. "Verification of Color Vegetation Indices for Automated Crop Imaging Applications." *Computers and Electronics in Agriculture* 63 (2): 282–293. doi:[10.1016/j.compag.2008.03.009](https://doi.org/10.1016/j.compag.2008.03.009).
- Motohka, T., K. N. Nasahara, H. Oguma, and S. Tsuchida. 2010. "Applicability of Green-Red Vegetation Index for Remote Sensing of Vegetation Phenology." *Remote Sensing* 2 (10): 2369–2387. doi:[10.3390/rs2102369](https://doi.org/10.3390/rs2102369).
- Muchiri, N., and S. Kimathi. 2016. "A Review of Applications and Potential Applications of UAV." *Proceedings of Sustainable Research and Innovation Conference* 0 (0): 280–283.
- Navia, J., I. Mondragon, D. Patino, and J. Colorado (2016). Multispectral Mapping in Agriculture: Terrain Mosaic Using an Autonomous Quadcopter UAV. In 2016 International Conference on Unmanned Aircraft Systems (ICUAS) (pp. 1351–1358). Retrieved from http://ieeexplore.ieee.org/xpls/abs_all.jsp?arnumber=7502606
- Nebiker, S., A. Annen, M. Scherrer, and D. Oesch. 2008. "A Light-Weight Multispectral Sensor for Micro UAV—Opportunities for Very High Resolution Airborne Remote Sensing." *The International Archives of the Photogrammetry, Remote Sensing and Spatial Information Sciences* 37(B1): 1193–1199.
- Nebiker, S., N. Lack, M. Abächerli, and S. Läderach (2016). Light-Weight Multispectral UAV Sensors and Their Capabilities for Predicting Grain Yield and Detecting Plant Diseases. *ISPRS-International Archives of the Photogrammetry, Remote Sensing and Spatial Information Sciences*, 963–970.
- Neto, J. C. (2004). A Combined Statistical-Soft Computing Approach for Classification and Mapping Weed Species in Minimum -Tillage Systems. ResearchGate. Retrieved from https://www.researchgate.net/publication/280148076_A_combined_statistical-soft_computing_approach_for_classification_and_mapping_weed_species_in_minimum_-tillage_systems
- Nex, F., and F. Remondino. 2013. "UAV for 3D Mapping Applications: A Review." *Applied Geomatics* 6 (1): 1–15. doi:[10.1007/s12518-013-0120-x](https://doi.org/10.1007/s12518-013-0120-x).

- Nolan, A. P., S. Park, M. O'connell, S. Fuentes, D. Ryu, and H. Chung (2015). Automated Detection and Segmentation of Vine Rows Using High Resolution UAS Imagery in a Commercial Vineyard. Presented at the 21st International Congress on Modelling and Simulation, Gold Coast, Australia. Retrieved from https://www.researchgate.net/profile/Mark_Oconnell/publication/284206199_Automated_detection_and_segmentation_of_vine_rows_using_high_resolution_UAS_imagery_in_a_commercial_vineyard/links/566e1c9f08ae1a797e405f39.pdf
- Otsu, N. 1979. "A Threshold Selection Method from Gray-Level Histograms." *IEEE Transactions on Systems, Man, and Cybernetics* 9 (1): 62–66. doi:10.1109/TSMC.1979.4310076.
- Pajares, G. 2015. "Overview and Current Status of Remote Sensing Applications Based on Unmanned Aerial Vehicles (UAVs)." *Photogrammetric Engineering & Remote Sensing* 81 (4): 281–329. doi:10.14358/PERS.81.4.281.
- Pappalardo, J. (2015). Unmanned Aircraft "Roadmap" Reflects Changing Priorities. Retrieved July 7, 2016, from http://www.nationaldefensemagazine.org/archive/2005/April/Pages/Unmanned_Aircraft5815.aspx
- Park, S., A. Nolan, D. Ryu, S. Fuentes, E. Hernandez, H. Chung, and M. O'connell (2015). Estimation of Crop Water Stress in a Nectarine Orchard Using High-Resolution Imagery from Unmanned Aerial Vehicle (UAV). In *International Congress on Modelling and Simulation (MODSIM)* (Tony Weber and Malcolm McPhee 29 November 2015 to 04 December 2015) (pp. 1413–1419). Modelling and Simulation Society of Australia and New Zealand. Retrieved from https://www.researchgate.net/profile/Sigfredo_Fuentes/publication/298070136_park/links/56e5daa008ae68afa112b648.pdf
- Peña, J. M., J. Torres-Sánchez, A. I. Castro, M. De, Kelly, and F. López-Granados. 2013. "Weed Mapping in Early-Season Maize Fields Using Object-Based Analysis of Unmanned Aerial Vehicle (UAV) Images." *PLoS One* 8 (10): e77151. doi:10.1371/journal.pone.0077151.
- Perez, A. J., F. Lopez, J. V. Benlloch, and S. Christensen. 2000. Colour and Shape Analysis Techniques for Weed Detection in Cereal Fields. In *Computers and Electronics in Agriculture* 25(3): 197–212. Elsevier. Retrieved from: <http://cat.inist.fr/?aModele=afficheN&cpsidt=1386838>.
- Pölönen, I., H. Saari, J. Kaivosoja, E. Honkavaara, and L. Pesonen (2013). Hyperspectral Imaging Based Biomass and Nitrogen Content Estimations from Light-Weight UAV. In *SPIE Remote Sensing* (p. 88870J–88870J). International Society for Optics and Photonics. Retrieved from <http://proceedings.spiedigitallibrary.org/proceeding.aspx?articleid=1757263>
- Poulton, C. V., and M. R. Watts. (2016). MIT and DARPA Pack Lidar Sensor Onto Single Chip. Retrieved August 4, 2016, from <http://spectrum.ieee.org/tech-talk/semiconductors/optoelectronics/mit-lidar-on-a-chip>
- Primicerio, J., S. F. Di Gennaro, E. Fiorillo, L. Genesio, E. Lugato, A. Matese, and F. P. Vaccari. 2012. "A Flexible Unmanned Aerial Vehicle for Precision Agriculture." *Precision Agriculture* 13 (4): 517–523. doi:10.1007/s11119-012-9257-6.
- Qi, J., A. Chehbouni, A. R. Huete, Y. H. Kerr, and S. Sorooshian. 1994. "A Modified Soil Adjusted Vegetation Index." *Remote Sensing of Environment* 48 (2): 119–126. doi:10.1016/0034-4257(94)90134-1.
- Quater, P. B., F. Grimaccia, S. Leva, M. Mussetta, and M. Aghaei. 2014. "Light Unmanned Aerial Vehicles (UAVs) for Cooperative Inspection of PV Plants." *IEEE Journal of Photovoltaics* 4 (4): 1107–1113. doi:10.1109/JPHOTOV.2014.2323714.
- Quiroz, R. (2015). Remote Sensing As a Monitoring Tool for Cropping Area Determination in Smallholder Agriculture in Tanzania and Uganda. Retrieved from <https://cgspace.cgiar.org/handle/10568/69110>
- Ramasamy, S., R. Sabatini, A. Gardi, and J. Liu. 2016. "LIDAR Obstacle Warning and Avoidance System for Unmanned Aerial Vehicle Sense-and-Avoid." *Aerospace Science and Technology* 55: 344–358. doi:10.1016/j.ast.2016.05.020. Retrieved from: <http://www.sciencedirect.com/science/article/pii/S1270963816301900>.
- Richards, J. A., and X. Jia. 2006. *Remote Sensing Digital Image Analysis: An Introduction*. 4th ed. Berlin: Springer.
- Riggs, G. A., D. K. Hall, and V. V. Salomonson. 1994. "A Snow Index for the Landsat Thematic Mapper and Moderate Resolution Imaging Spectroradiometer." In *Geoscience and Remote*

- Sensing Symposium, 1994. IGARSS '94. International Surface and Atmospheric Remote Sensing: Technologies, Data Analysis and Interpretation* 4:1942–1944. doi:[10.1109/IGARSS.1994.399618](https://doi.org/10.1109/IGARSS.1994.399618).
- Rokhmana, C. A. 2015. "The Potential of UAV-based Remote Sensing for Supporting Precision Agriculture in Indonesia." *Procedia Environmental Sciences* 24: 245–253. doi:[10.1016/j.proenv.2015.03.032](https://doi.org/10.1016/j.proenv.2015.03.032).
- Rondeaux, G., M. Steven, and F. Baret. 1996. "Optimization of Soil-Adjusted Vegetation Indices." *Remote Sensing of Environment* 55 (2): 95–107. doi:[10.1016/0034-4257\(95\)00186-7](https://doi.org/10.1016/0034-4257(95)00186-7).
- Rouse, J. W. JR, R. H. Haas, J. A. Schell, and D. W. Deering. 1974. "Monitoring Vegetation Systems in the Great Plains with ERTS." *NASA Special Publication* 351: 309.
- Saari, H., I. Pellikka, L. Pesonen, S. Tuominen, J. Heikkilä, C. Holmlund, ... T. Antila. 2011. "Unmanned Aerial Vehicle (UAV) Operated Spectral Camera System for Forest and Agriculture Applications." In *Remote Sensing for Agriculture, Ecosystems, and Hydrology XIII* 8174: 81740H–81740H–15. doi:[10.1117/12.897585](https://doi.org/10.1117/12.897585).
- Salamí, E., C. Barrado, and E. Pastor. 2014. "UAV Flight Experiments Applied to the Remote Sensing of Vegetated Areas." *Remote Sensing* 6 (11): 11051–11081. doi:[10.3390/rs6111051](https://doi.org/10.3390/rs6111051).
- Siebert, S., and J. Teizer. 2014. "Mobile 3D Mapping for Surveying Earthwork Projects Using an Unmanned Aerial Vehicle (UAV) System." *Automation in Construction* 41: 1–14. doi:[10.1016/j.autcon.2014.01.004](https://doi.org/10.1016/j.autcon.2014.01.004).
- Simelli, I., and A. Tsagaris (2015). The Use of Unmanned Aerial Systems (UAS) in Agriculture. Presented at the 7th International Conference on Information and Communication Technologies in Agriculture, Food and Environment (HAICTA 2015), Kavala, Greece.
- Sullivan, J. M. 2006. "Evolution or Revolution? The Rise of UAVs." *IEEE Technology and Society Magazine* 25 (3): 43–49. doi:[10.1109/MTAS.2006.1700021](https://doi.org/10.1109/MTAS.2006.1700021).
- Suomalainen, J., N. Anders, S. Iqbal, G. Roerink, J. Franke, P. Wenting, ... L. Kooistra. 2014. "A Lightweight Hyperspectral Mapping System and Photogrammetric Processing Chain for Unmanned Aerial Vehicles." *Remote Sensing* 6 (11): 11013–11030. doi:[10.3390/rs6111013](https://doi.org/10.3390/rs6111013).
- Thenkabail, P. S., R. B. Smith, and E. De Pauw. 2000. "Hyperspectral Vegetation Indices and Their Relationships with Agricultural Crop Characteristics." *Remote Sensing of Environment* 71 (2): 158–182. doi:[10.1016/S0034-4257\(99\)00067-X](https://doi.org/10.1016/S0034-4257(99)00067-X).
- Thiel, C., and C. Schmullius. 2016. "Comparison of UAV Photograph-Based and Airborne LiDAR-Based Point Clouds Over Forest from a Forestry Application Perspective." *International Journal of Remote Sensing* 0 (0): 1–16. doi:[10.1080/01431161.2016.1225181](https://doi.org/10.1080/01431161.2016.1225181).
- Torres-Sánchez, J., F. López-Granados, and J. M. Peña. 2015. "An Automatic Object-Based Method for Optimal Thresholding in UAV Images: Application for Vegetation Detection in Herbaceous Crops." *Computers and Electronics in Agriculture* 114: 43–52. doi:[10.1016/j.compag.2015.03.019](https://doi.org/10.1016/j.compag.2015.03.019).
- Torres-Sánchez, J., J. M. Peña, A. I. De Castro, and F. López-Granados. 2014. "Multi-Temporal Mapping of the Vegetation Fraction in Early-Season Wheat Fields Using Images from UAV." *Computers and Electronics in Agriculture* 103: 104–113. doi:[10.1016/j.compag.2014.02.009](https://doi.org/10.1016/j.compag.2014.02.009).
- Tucker, C. J. 1979. "Red and Photographic Infrared Linear Combinations for Monitoring Vegetation." *Remote Sensing of Environment* 8 (2): 127–150. doi:[10.1016/0034-4257\(79\)90013-0](https://doi.org/10.1016/0034-4257(79)90013-0).
- Turner, D., A. Lucieer, and C. Watson (2011). Development of an Unmanned Aerial Vehicle (UAV) for Hyper Resolution Vineyard Mapping Based on Visible, Multispectral, and Thermal Imagery, In *Proceedings of 34th International symposium on remote sensing of environment* (p. 4).
- Turner, D., A. Lucieer, and C. Watson. 2012. "An Automated Technique for Generating Georectified Mosaics from Ultra-High Resolution Unmanned Aerial Vehicle (UAV) Imagery, Based on Structure from Motion (SfM) Point Clouds." *Remote Sensing* 4 (12): 1392–1410. doi:[10.3390/rs4051392](https://doi.org/10.3390/rs4051392).
- Turner, W., S. Spector, N. Gardiner, M. Fladeland, E. Sterling, and M. Steininger. 2003. "Remote Sensing for Biodiversity Science and Conservation." *Trends in Ecology & Evolution* 18 (6): 306–314. doi:[10.1016/S0169-5347\(03\)00070-3](https://doi.org/10.1016/S0169-5347(03)00070-3).
- Uto, K., H. Seki, G. Saito, and Y. Kosugi. 2013. "Characterization of Rice Paddies by a UAV-Mounted Miniature Hyperspectral Sensor System." *IEEE Journal of Selected Topics in Applied Earth Observations and Remote Sensing* 6 (2): 851–860. doi:[10.1109/JSTARS.2013.2250921](https://doi.org/10.1109/JSTARS.2013.2250921).

- Wagner, M. 2015. Unmanned Aerial Vehicles (SSRNScholarly Paper No. ID 2584652). Rochester, NY: Social Science Research Network. Retrieved from. <http://papers.ssrn.com/abstract=2584652>.
- Wallace, L. (2013). Assessing the Stability of Canopy Maps Produced from UAV-LiDAR Data. In 2013 IEEE International Geoscience and Remote Sensing Symposium - IGARSS (pp. 3879–3882). doi:10.1109/IGARSS.2013.6723679
- Wallace, L., A. Lucieer, Z. Malenovsky, D. Turner, and P. Vopěnka. 2016. "Assessment of Forest Structure Using Two UAV Techniques: A Comparison of Airborne Laser Scanning and Structure from Motion (SfM) Point Clouds." *Forests* 7 (3): 62. doi:10.3390/f7030062.
- Wallace, L., A. Lucieer, C. Watson, and D. Turner. 2012. "Development of a UAV-LiDAR System with Application to Forest Inventory." *Remote Sensing* 4 (6): 1519–1543. doi:10.3390/rs4061519.
- Wallace, L., A. Lucieer, and C. S. Watson. 2014. "Evaluating Tree Detection and Segmentation Routines on Very High Resolution UAV LiDAR Data." *IEEE Transactions on Geoscience and Remote Sensing* 52 (12): 7619–7628. doi:10.1109/TGRS.2014.2315649.
- Wallace, L. O., A. Lucieer, D. Turner, and C. S. Watson (2011). Error Assessment and Mitigation for Hyper-Temporal UAV-Borne LiDAR Surveys of Forest Inventory. Presented at the SilviLaser 2011, Hobart, Tasmania. Retrieved from <http://events.cdesign.com.au/ei/viewpdf.esp?id=297&file=P:/Eventwin/docs/pdf/silvi2011Abstract00033.pdf>
- Ward, S., J. Hensler, B. Alsalam, and L. F. Gonzalez (2016). Autonomous UAVs Wildlife Detection Using Thermal Imaging, Predictive Navigation and Computer Vision. In Australian Research Centre for Aerospace Automation; School of Electrical Engineering & Computer Science; Institute for Future Environments; Science & Engineering Faculty. Yellowstone Conference Center, Big Sky, Montana. Retrieved from <http://eprints.qut.edu.au/92309/>
- Watts, A. C., V. G. Ambrosia, and E. A. Hinkley. 2012. "Unmanned Aircraft Systems in Remote Sensing and Scientific Research: Classification and Considerations of Use." *Remote Sensing* 4 (6): 1671–1692. doi:10.3390/rs4061671.
- Wehrhan, M., P. Rauneker, and M. Sommer. 2016. "UAV-Based Estimation of Carbon Exports from Heterogeneous Soil Landscapes—A Case Study from the CarboZALF Experimental Area." *Sensors* 16 (2): 255. doi:10.3390/s16020255.
- Woebbecke, D. M., G. E. Meyer, K. Von Bargen, and D. A. Mortensen (1995). Color Indices for Weed Identification under Various Soil, Residue, and Lighting Conditions. *Transactions of the ASAE (USA)*. Retrieved from <http://agris.fao.org/agris-search/search.do?recordID=US9561468>
- Xu, H. 2006. "Modification of Normalised Difference Water Index (NDWI) to Enhance Open Water Features in Remotely Sensed Imagery." *International Journal of Remote Sensing* 27 (14): 3025–3033. doi:10.1080/01431160600589179.
- Zarco-Tejada, P. J., A. Berjón, R. López-Lozano, J. R. Miller, P. Martín, V. Cachorro, ... A. De Frutos. 2005. "Assessing Vineyard Condition with Hyperspectral Indices: Leaf and Canopy Reflectance Simulation in a Row-Structured Discontinuous Canopy." *Remote Sensing of Environment* 99 (3): 271–287. doi:10.1016/j.rse.2005.09.002.
- Zarco-Tejada, P. J., V. González-Dugo, and J. A. Berni. 2012. "Fluorescence, Temperature and Narrow-Band Indices Acquired from a UAV Platform for Water Stress Detection Using a Micro-Hyperspectral Imager and a Thermal Camera." *Remote Sensing of Environment* 117: 322–337. doi:10.1016/j.rse.2011.10.007.
- Zhang, C., and J. M. Kovacs. 2012. "The Application of Small Unmanned Aerial Systems for Precision Agriculture: A Review." *Precision Agriculture* 13 (6): 693–712. doi:10.1007/s11119-012-9274-5.